NACA

RESEARCH MEMORANDUM

for the

Air Materiel Command, U.S. Air Forces

WIND-TUNNEL INVESTIGATION OF THE LOW-SPEED CHARACTERISTICS OF A 1/8-SCALE MODEL OF THE REPUBLIC XP-91 AIRPLANE WITH A VEE AND A CONVENTIONAL TAIL. ADDENDUM - CHARACTERISTICS WITH A REVISED CONVENTIONAL TAIL AND DROOPED WING TIPS

By James A. Weiberg and Warren E. Anderson

Ames Aeronautical Laboratory
Moffett Field, Calif.

[redacted]

NATIONAL ADVISORY COMMITTEE FOR AERONAUTICS

WASHINGTON

JAN 2 1948

NATIONAL ADVISORY COMMITTEE FOR AERONAUTICS

RESEARCH MEMORANDUM

for the

Air Materiel Command, U.S. Air Forces

WIND-TUNNEL INVESTIGATION OF THE LOW-SPEED CHARACTERISTICS OF A 1/8-SCALE MODEL OF THE REPUBLIC XP-91 AIRPLANE WITH A VEE AND A CONVENTIONAL TAIL. ADDENDUM - CHARACTERISTICS WITH A REVISED CONVENTIONAL TAIL AND DROOPED WING TIPS

By James A. Weiberg and Warren E. Anderson

SUMMARY

Additional wind-tunnel tests were made of a 1/8-scale model of the Republic XP-91 airplane to determine its characteristics with various modifications. The modifications included a revised conventional tail, revised rocket arrangement, drooped wing tips, and revised landing gear and doors. Tests were also made to determine the effectiveness of the control surfaces of the model with the conventional tail and the effect of changing wing incidence and tail length.

The revised rocket arrangement provided a considerable increase in the static directional stability contributed by the vee tail at small angles of yaw. The conventional tail provided a greater static directional stability than the vee tail without increasing the rolling moment due to sideslip.

The rolling moment due to sideslip was considerably reduced by either drooped wing tips or open main landing-gear doors. The reduction in rolling moment due to sideslip resulting from the drooped tips was less with the landing-gear doors open than with the doors closed.

A change in wing incidence from 0° to 6° reduced the elevator angle required for balance by approximately 6°.

INTRODUCTION

Preliminary tests of a 1/8-scale model of the Republic XP-91 airplane were reported in reference 1. As a result of those tests, the model was modified and additional tests were made. The modifications included a new conventional tail revised rocket arrangement, revised landing gear and doors, and drooped wing tips. Tests were also made to recheck the effectiveness of the vee tail and to determine the control-surface characteristics.

The tests were made in one of the Ames 7- by 10-foot wind tunnels during the period from October 2 – 16, 1947. During the testing the Republic Aviation Corporation was represented by Mr. Robert B. Liddell.

DESCRIPTION OF THE MODEL AND THE AIRPLANE

The Republic XP-91 airplane is a single-place interceptor having a swept-back wing with inverse taper and swept-back tail surfaces. Further description of the airplane is given in reference 1.

The general arrangement of the airplane with the vee and the conventional tails utilized in these tests is shown in figure 1, and the major airplane dimensions are given in table I. Dimensions of the control surfaces are given in table II. Deflections were measured in planes perpendicular to the control hinge lines. The two tails tested on the model are shown in figure 2.

Subsequent to the tests of reference 1, the conventional tail was redesigned by the Republic Aviation Corporation and the four rockets at the rear of the fuselage were rearranged. The relative sizes of the rocket fairings for these tests and those of reference 1 are shown in figure 3. For the tests with the vee tail, the upper rocket fairing was removed. The side area of the revised lower rocket fairing is approximately 15.5 percent of the vertical projected area of the vee tail.

The vee tail used in the tests reported herein had a slightly larger span than the vee tail of reference 1, resulting in 6-percent greater area. Except for this difference in span, the geometry of the two vee tails was the same.

To reduce the roll due to sideslip with flaps and gear down, the main landing-gear doors were left open when the gear was lowered. The doors (figs. 4 and 5) were opened 125° and had a total area of 28 square feet (full scale) or 8.7 percent of the wing area. Their hinges were 91 percent of the semispan from the center of the wing with the plain tips. These doors differed from those of reference 1 in shape, size, and angle of opening. A comparison of the doors may be obtained from figure 4 of this report and figure 12 of reference 1.

Negative dihedral was incorporated in the wing tips of the model by increasing the span 9 percent and drooping the outer 14 percent of this span as shown in figures 1 and 4. The wing area was thus increased 8 percent.

The model tested (figs. 6 to 10) represented the airplane to one eighth scale with the following exceptions:

1. The air inlet in the fuselage nose was faired over, adding 1.67 feet (full scale) to the fuselage length.

2. The external wing tanks and nose-wheel doors were omitted.

3. The wing dihedral on the model was -5.5° instead of -5.0°.

4. Only the right wing panel incorporated an aileron.

5. The control-surface balances were not simulated but the control-surface leading-edge gaps were scaled during the tests.

The model was mounted in the tunnel on a single strut (fig. 11). Rolling and pitching moments were measured by resistance-type electrical strain gages within the model. All other forces and moments were measured by the wind-tunnel balance system.

SYMBOLS AND COEFFICIENTS

All data are presented as standard NACA coefficients corrected for support tares, tunnel-wall interference, and stream inclination. Corrections for tunnel-wall interference and stream inclination are given in the appendix of reference 1. All force coefficients are referred to the wind axes. Yawing- and pitching-moment coefficients are given about the stability axes and rolling-moment coefficients about the body axes.[1] These systems of axes[2] are each composed of three mutually perpendicular axes with their origins at a center of gravity of the airplane located on the fuselage reference line and 18 percent of the M.A.C. aft of the M.A.C. leading edge.

---

[1]If rolling moments are transferred to the stability axes, they are reduced by approximately 2 percent at an angle of attack of 12° and 0 percent at an angle of attack of 0°.

[2]These axes are defined in reference 1.

All force and moment coefficients, including those for the tests with the drooped wing tips (by which the wing area was increased 8 percent), are based on the dimensions of the wing with plain tips as given in table I.

The angle of attack is referred to the wing reference plane, which contains the fuselage reference line when the wing incidence is 0°. The angle of yaw is referred to the plane of symmetry.

Coefficients and symbols used throughout the report are defined in the appendix.

RESULTS AND DISCUSSION

The test data for the model were obtained at the following Reynolds numbers:

1. R = 1,100,000 for the tests to obtain the lateral characteristics with high angles of yaw ($\pm 14^\circ$) and the longitudinal characteristics.

2. R = 1,600,000 for the tests to obtain the lateral characteristics within a limited yaw range ($\pm 6^\circ$).

The results of the preliminary tests of the model reported in reference 1 indicate that the effect of Reynolds number on the aerodynamic characteristics was negligible within the limited range of Reynolds numbers available. The full-scale Reynolds number at 120 miles per hour is approximately 12,000,000.

Characteristics of the Model with the Conventional Tail

The lateral characteristics of the model with the conventional tail and plain wing tips are presented in figure 12. Test data are presented for several angles of attack and include measurements obtained with the flaps and gear retracted (fig. 12(a)), and with the flaps and gear extended with the main landing-gear doors open (fig. 12(b)). The variations of the stability parameters[3] C_{n_ψ} and C_{l_ψ} with lift coefficient have been obtained from figure 12 and are presented in figure 13.

[3]Values of C_{n_ψ} and C_{l_ψ} were measured between approximately $\pm 2^\circ$ of yaw.

The directional-stability parameter C_{n_ψ}, as indicated by figure 13, was approximately -0.0032 and -0.0037 for the model with flaps and gear retracted and extended, respectively, at low lift coefficients, and became slightly less negative at the higher lift coefficients.

The rolling moment due to sideslip, as indicated by C_{l_ψ} in figure 13, increased with an increase of lift coefficient and reached maximum values of 0.0039 at a C_L of 0.47 for flaps and gear retracted and 0.0027 at a C_L of 0.85 for flaps and gear extended. Reference 2 indicates that large increases of Reynolds number may tend to increase C_{l_ψ} at high lift coefficients so that, for the full-scale airplane, the maximum values of C_{l_ψ} may be even higher than those indicated by figure 13.

Characteristics of the Model with the Vee Tail

Since the rear of the fuselage had been changed to conform to a revised rocket arrangement (fig. 3), tests were made to determine whether the effectiveness of the vee tail was altered.

The lateral characteristics of the model with the vee tail are shown in figures 14 and 15 for the model with the flaps and gear retracted and extended, respectively. Similar data for the model with the tail removed and the flaps and gear extended are presented in figure 16. Data are presented for several angles of attack. From figures 14, 15, and 16, the variations of the directional-stability parameter[4] C_{n_ψ} with lift coefficient have been obtained and are presented in figure 17. Also included are data for the vee tail of reference 1. This figure shows that C_{n_ψ} was considerably affected by the shape of the rear of the fuselage. The addition of the lower rocket fairing resulted in a change in C_{n_ψ} of -0.0011, which was nearly constant with lift coefficient and unaffected by flap deflection. With the rockets removed there was a difference in C_{n_ψ} for the model with the vee tail of the present tests and the vee tail of reference 1. This difference in C_{n_ψ} can be attributed to the directional stability contributed by the landing-gear doors which will be discussed later.

[4] Values of C_{n_ψ} were measured between ±2° of yaw.

Beyond the ±2° range of angle of yaw, C_{n_ψ} was relatively unaffected by the shape of the rear of the fuselage, as may be seen from figure 18.[5] The contribution of the lower rocket fairing to the directional stability of the model with the tail removed was negligible (fig. 12).

The results of tests of the model with the vee tail (lower rocket fairing on) to determine the effect on static stability of increasing the tail length from 1.5 to 2.0 M.A.C. (0.51 to 0.68 spans) are presented in figure 19. The tail locations tested may be seen in figures 8 and 9. Figure 19 shows that the change in tail length gave a change in directional stability C_{n_ψ} of −0.0003. This change in C_{n_ψ} is only 20 percent of that expected. However, the test data have been checked and no errors of computation have been found.

Comparative Effectiveness of the Vee and Conventional Tails

A comparison of the lateral characteristics of the model with the vee and conventional tails with the flaps and gear retracted and extended is shown in figure 13. This figure shows the variation with lift coefficient of the stability parameters C_{n_ψ} and C_{l_ψ} obtained from figures 12, 14, 15, and 16. Both the vee and the conventional tails produced nearly the same rolling moment due to sideslip. The directional stability of the model, however, was greater with the conventional tail than with the vee tail. At a lift coefficient of 0.5 C_{n_ψ} of the model with flaps and gear both retracted and extended was more negative by 0.0010 with the conventional tail than with the vee tail.

Effects of Landing-Gear Doors

To evaluate the effects of the main landing-gear doors (figs. 4 and 5) on the lateral characteristics of the model, tests with the conventional tail and plain wing tips were made with the landing-gear doors open (fig. 12(b)) and closed (fig. 20). The effect of the doors on the variation of C_{n_ψ} and C_{l_ψ} with lift coefficient is presented in figure 21. These data show that the doors reduced C_{l_ψ} by 0.0019 regardless of lift coefficient and also changed C_{n_ψ} by −0.0006 at a lift coefficient of 0.6.

[5]The experimental points have been omitted from figure 12 for clarity.

Effect of Drooped Wing Tips

The results of tests to determine the effect of the drooped wing tips on the lateral characteristics of the model are presented in figure 22. The variations of C_{n_ψ} and C_{l_ψ} with lift coefficient have been obtained from figure 22 and are presented in figure 21 for comparison with similar data for the model with plain wing tips. The drooped tips reduced the maximum value of C_{l_ψ} by 0.0017. Although this reduction was less than that obtained from the landing-gear doors, the variation of C_{l_ψ} with lift coefficient was less for the model with the drooped wing tips than with the plain tips.

Figure 21 shows that when the landing-gear doors were open with the drooped wing tips on the model there was a mutual interference between the doors and tips such that the reduction in maximum C_{l_ψ} resulting from the drooped tips was less with the doors open than with the doors closed. The drooped wing tips also increased the directional stability C_{n_ψ} by 0.0003 at a lift coefficient of 0.7.

The effect of the drooped wing tips on the longitudinal characteristics is shown in figure 23. This figure shows that, with flaps and gear up, the drooped tips increased the lift coefficient (based on the original area) at a given angle of attack by an amount which varied from 0 at 0° angle of attack to 0.13 at maximum lift. The drooped tips also resulted in an increase in the static longitudinal stability of the model at low lift coefficients.

With the flaps and gear down and the landing-gear doors open, the mutual interference between the doors and the drooped wing tips reduced the increment in lift coefficient obtained from the tips. The drooped tips increased the static longitudinal stability of the model with the flaps and gear down at low lift coefficients, but the increase was not as large as that with flaps and gear up.

Effect of Wing Incidence

To adjust the longitudinal balance on the XP-91 airplane, the wing incidence is varied in flight from 0° for high-speed level flight to 6° for landing. This results in a change in downwash at the tail and, consequently, in the lift coefficient for balance. This change in longitudinal balance for the model with the conventional tail and with the flaps and gear down is shown in figure 24. When the wing incidence was changed from 0° to 6° the model pitching moments were changed sufficiently to reduce the up-elevator deflection required for balance by approximately 6° with almost no change in static longitudinal stability. The rotation of the fuselage relative to the wing when the incidence was changed reduced the lift coefficient 0.1 for a constant wing angle of attack.

The lateral characteristics of the model with 6° wing incidence are shown in figure 25 for the model with the conventional tail and with the flaps and gear down. Comparison of this figure with figure 12(b) shows that the lateral characteristics of the model were relatively unaffected by the change in incidence.

Control-Surface Effectiveness

Aileron control.- Tests were made to determine whether the aileron effectiveness during sideslip was affected by the drooped wing tips. Data were obtained through ±6° of yaw at two angles of attack, 0° and 8°, for the model with the flaps and gear down and the landing-gear doors open. The tests were made with the aileron on the right wing panel deflected ±20°.

The results of the tests of the model with plain and drooped wing tips are presented in figure 26. This figure shows that the rolling moment due to aileron deflection in sideslips was relatively unaffected by the drooped wing tips. However, interference between the ailerons and the landing gear and doors may have obscured any effects due to the tips.

Elevator control. The results of tests to determine the effectiveness of the elevators on the conventional tail are shown in figure 27. The elevator effectiveness as indicated by $dC_m/d\delta_e$ was −0.009 and −0.008 with the flaps and gear retracted and extended, respectively. These values are for lift coefficients from 0 to 0.5 and for ±10° elevator deflections.

Rudder control.- Rudder-control characteristics of the model with the conventional tail are shown in figure 28 for the model with the flaps up and with the flaps and gear down at two angles of attack. These data indicate that with 0° yaw $dC_n/d\delta_r$ was −0.0021 and was relatively constant with model attitude and flap deflection. Figure 28 indicates that a rudder deflection of 20° (maximum) balanced the model with approximately 12° of sideslip.

Stabilizer effectiveness.- The effectiveness of the horizontal stabilizer is shown in figure 29(a) and 29(b) as functions of lift coefficient and angle of attack, respectively. The data of figure 29(b) indicate that $dC_m/d\alpha_T$ was -0.018 and was relatively unaffected by flap deflection.

CONCLUSIONS

From the foregoing discussion of the results of tests of a 1/8-scale model of the Republic XP-91 airplane, the following may be concluded:

1. The shape of the fuselage near the tail had a considerable effect on the yawing moment produced by the vee tail.

2. The model was more stable directionally with the conventional tail than with the vee tail without increasing the rolling moment due to sideslip.

3. The rolling moment due to sideslip was reduced by either drooped wing tips or open main landing-gear doors. Because of a mutual interference between the drooped tips and the doors, the reduction in rolling moment due to sideslip resulting from the drooped tips was less with the doors open than with the doors closed.

4. Increasing the wing incidence from 0° to 6° reduced the up-elevator deflection required for balance by approximately 8°.

5. The aileron effectiveness with sideslip for the model with the flaps and gear down and the landing-gear doors open was relatively unaffected by the drooped wing tips.

Ames Aeronautical Laboratory,
National Advisory Committee for Aeronautics,
Moffett Field, Calif.

APPENDIX

Coefficients and Symbols

The symbols and coefficients used throughout the report are defined below:

C_L lift coefficient $\left(\frac{\text{lift}}{qS_w}\right)$

C_y side-force coefficient $\left(\frac{\text{side force}}{qS_w}\right)$

C_l rolling-moment coefficient $\left(\frac{\text{rolling moment}}{qS_w b_w}\right)$

C_m pitching-moment coefficient $\left(\frac{\text{pitching moment}}{qS_w \bar{c}_w}\right)$

C_n yawing-moment coefficient $\left(\frac{\text{yawing moment}}{qS_w b_w}\right)$

C_{n_ψ} rate of change of yawing moment with angle of yaw $(dC_n/d\psi)$, degrees

C_{l_ψ} rate of change of rolling moment with angle of yaw $(dC_l/d\psi)$, degrees

C_{m_0} C_m at $C_L = 0$

A aspect ratio

b span, feet

c chord, feet

$\bar{c}$ mean aerodynamic chord, feet

i incidence, degrees

l_T tail length from $0.25\bar{c}$ of wing to $0.25\bar{c}$ of tail, feet

q dynamic pressure $(\frac{1}{2}\rho V^2)$, pounds per square foot

R Reynolds number

V	velocity, feet per second
α_u	geometric angle of attack of wing reference plane (uncorrected), degrees
α	angle of attack of wing reference plane corrected for tunnel-wall interference and stream inclination, degrees
Γ	dihedral, degrees
δ	control-surface deflection, degrees
ρ	mass density of air, slugs per cubic foot
ψ	angle of yaw of fuselage plane of symmetry, degrees

Subscripts:

a_r	right aileron
e	elevator
r	rudder
T	tail
w	wing

REFERENCES

1. Weiberg, James A., and Anderson, Warren E.: Wind-Tunnel Investigation of the Low-Speed Characteristics of a 1/8-Scale Model of the Republic XP-91 Airplane with a Vee and a Conventional Tail. NACA CRM No. SA7L07, 1947.

2. Salmi, Reino J., Conner, D. William, and Graham, Robert R.: Effects of a Fuselage on the Aerodynamic Characteristics of a 42° Sweptback Wing at Reynolds Numbers to 8,000,000. NACA RRM No. L7E13, 1947.

TABLE I.- BASIC DIMENSIONS OF THE REPUBLIC XP-91 AIRPLANE AND VARIOUS TAILS

Item	Wing		Vee tail	Conventional tail	
	Plain tips	Drooped tips	Chord plane	Hori-zontal	Verti-cal
Area, sq ft	320	345.65	86.27	71.4	48.3
Span, ft	31.33	34.14	21.9[a]	16.66	9.75
Aspect ratio	3.07	3.31	5.57[a]	3.89	1.97
Taper ratio $\left(\frac{\text{tip chord}}{\text{root chord}}\right)$	1.625	- - -	1.0	1.0	.43
M.A.C., ft	10.59	- - -	3.94	4.29	5.21
Dihedral, deg	-5.5	- - -	38	0	- - -
Incidence, deg	Variable	- - -	0	0	- - -
Airfoil	Republic	- - -	- - -	- - -	- - -
Section	R4,45-1510-.9	- - -	- - -	- - -	- - -
Percent thickness (normal to leading edge)	7.6[b]	- - -	10	10	10[b]
Sweep of leading edge, deg	34.3	- - -	33.5	40	36.9
Tail length,[c] ft	- - -	- - -	16.4	17.5	15.5

[a]Measured in chord plane perpendicular to fuselage reference line.
[b]Measured parallel to fuselage reference line.
[c]$0.25\bar{c}$ wing to $0.25\bar{c}$ tail.

TABLE II.– DIMENSIONS OF THE MOVABLE SURFACES ON THE REPUBLIC XP-91 AIRPLANE

Dimension	Ailerons	Flaps	Elevators	Rudder
Area aft hinge line (both sides), sq ft	38.2	30.0	20.0	12.27
Span (one side), ft	6.11	6.23	7.75	8.64
Hinge-line location, percent chord	73	75	70	70

FIGURE LEGENDS

Figure 1.– General arrangement of the Republic XP-91 airplane. (a) With vee tail and plain wing tips. (b) With conventional tail, drooped wing tips.

Figure 2.– Tails tested on the 1/8-scale model of the Republic XP-91 airplane. (a) Vee tail. (b) Conventional tail.

Figure 3.– Comparison of the original and revised rocket arrangement.

Figure 4.– Plain wing tip of the model with landing-gear door open. (a) Rear view. (b) Side view.

Figure 5.– Drooped wing tip of the model with landing-gear door open. (a) Front view. (b) Rear view.

Figure 6.– The 1/8-scale model of the Republic XP-91 airplane with conventional tail and drooped wing tips, flaps and gear down, landing-gear doors open. (a) Front view. (b) Rear view.

Figure 7.– The conventional tail. (a) Plan view. (b) Side view.

Figure 8.– The vee tail in the forward position. (a) Plan view. (b) Side view.

Figure 9.– The vee tail in the aft position. (a) Plan view. (b) Side view.

Figure 10.– Rear portion of the fuselage with tail removed. (a) Lower rocket fairing on. (b) Lower rocket fairing off.

Figure 11.– Model support.

Figure 12.– Lateral characteristics with conventional tail, plain wing tips. (a) Flaps up.

Figure 12.– Concluded. (b) Flaps and gear down, landing-gear doors open 125°.

Figure 13.– Comparison of the lateral characteristics of the model with the vee and conventional tails, lower rocket fairing on, plain wing tips.

Figure 14.– Lateral characteristics with vee tail, flaps up, plain wing tips. (a) Lower rocket fairing on.

Figure 14.– Concluded. (b) Lower rocket fairing off.

Figure 26.– Aileron effectiveness with flaps and gear down, landing-gear doors open 125°, conventional tail. (a) Plain wing tips. (b) Drooped wing tips.

Figure 27.– Effectiveness of the elevators on the conventional tail, drooped wing tips. (a) Flaps up. (b) Flaps and gear down, landing-gear doors open 125°.

Figure 28.– Effectiveness of the rudder on the conventional tail, drooped wing tips. (a) Flaps up. (b) Flaps and gear down, landing-gear doors open 125°.

Figure 29.– Effect of stabilizer incidence on longitudinal characteristics, drooped wing tips, conventional tail. (a) Variation of α and C_m with C_L.

Figure 29.– Concluded. (b) Variation of C_m with α_u.

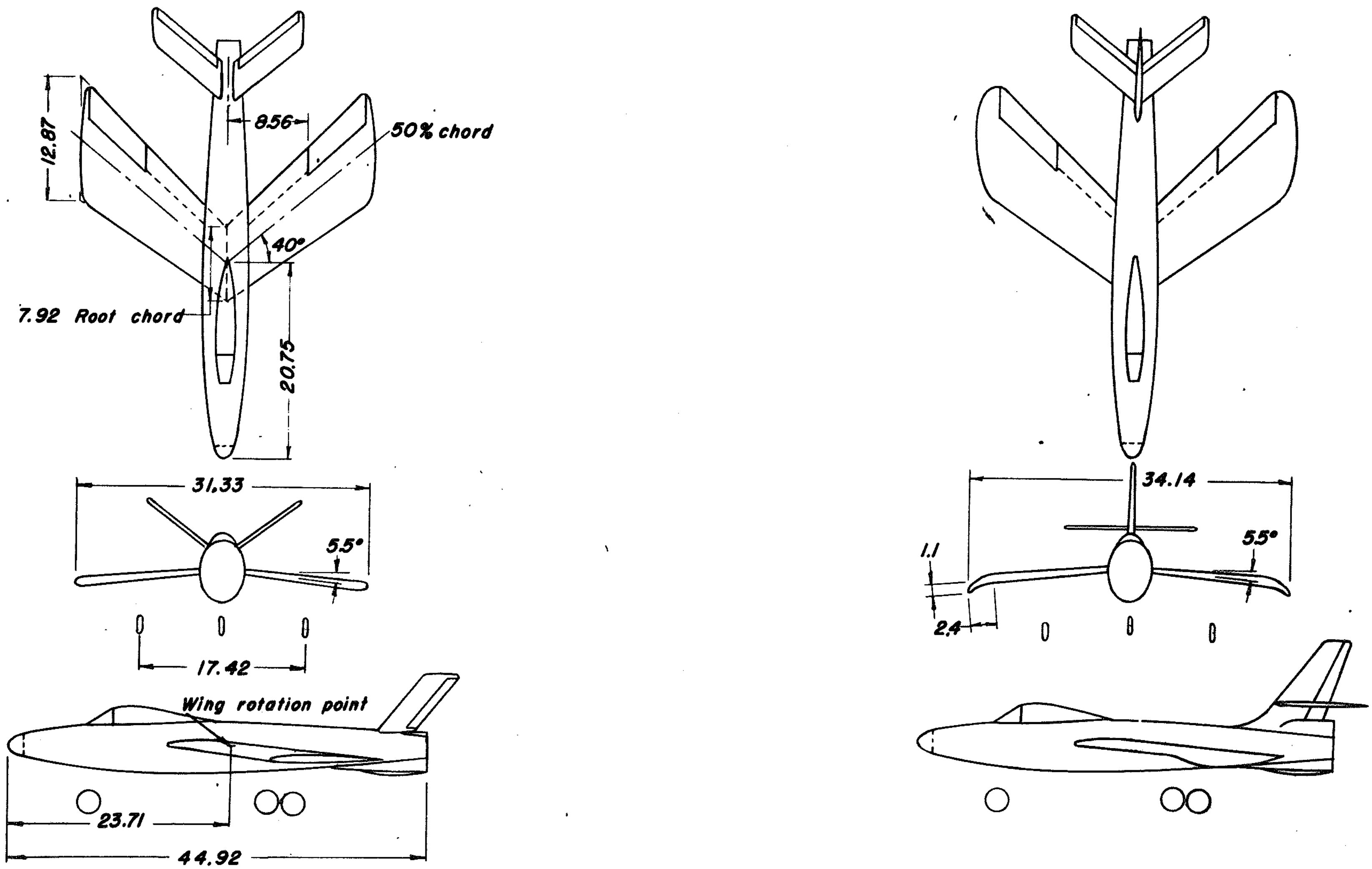

All dimensions feet full scale

(a) With vee tail and plain wing tips.

(b) With conventional tail, drooped wing tips.

Figure 1.- General arrangement of the Republic XP-91 Airplane.

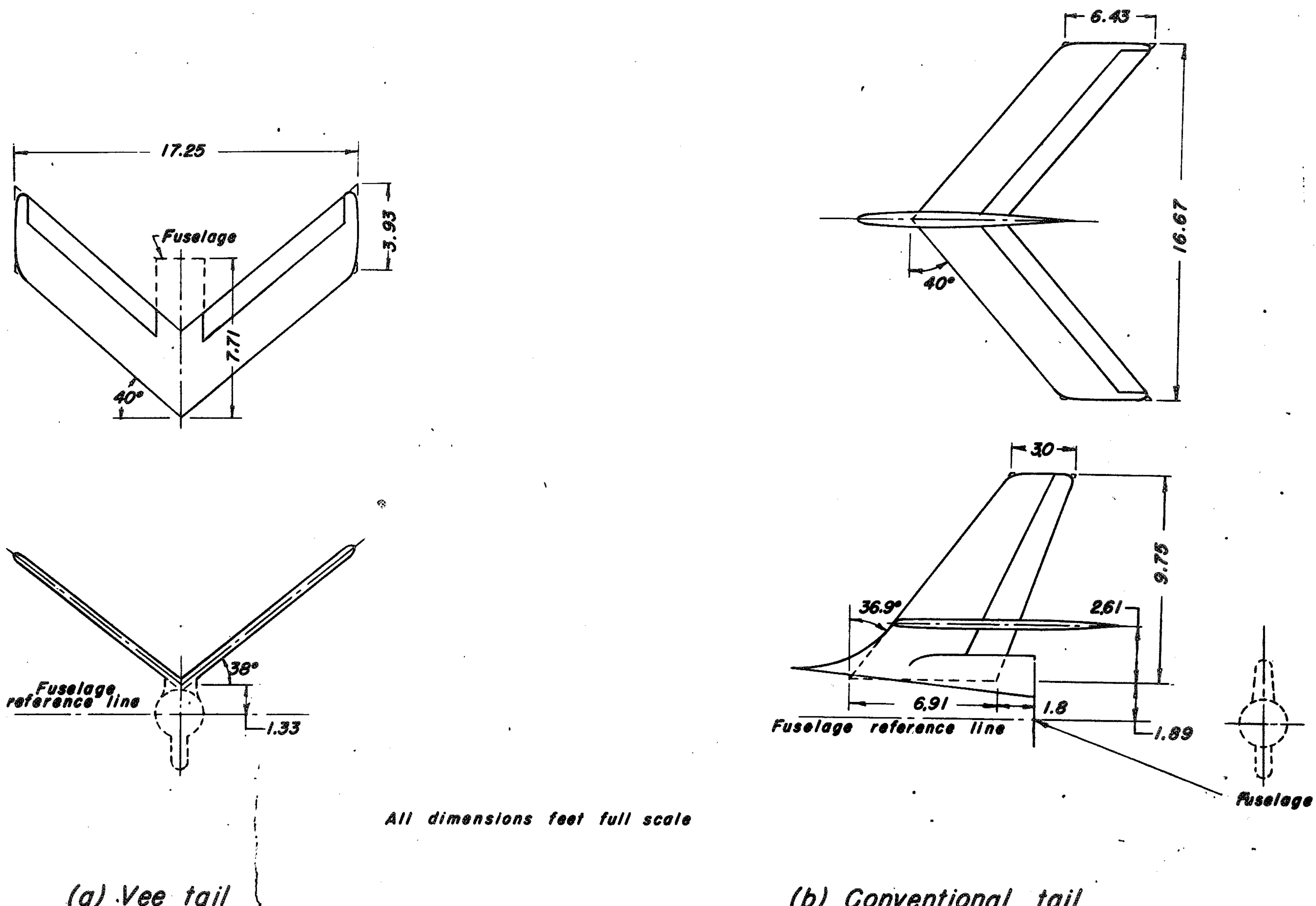

Figure 2.- Tails tested on the $\frac{1}{8}$-scale model of the Republic XP-91 Airplane.

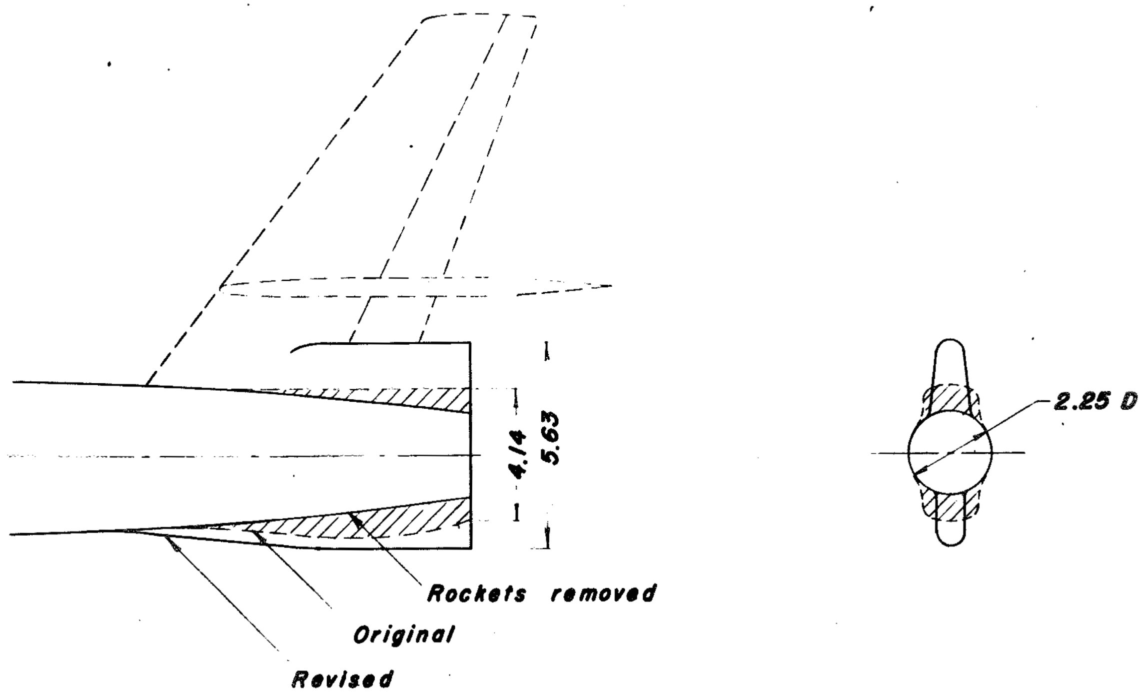

All dimensions feet full scale

Figure 3.- Comparison of the original and revised rocket arrangement.

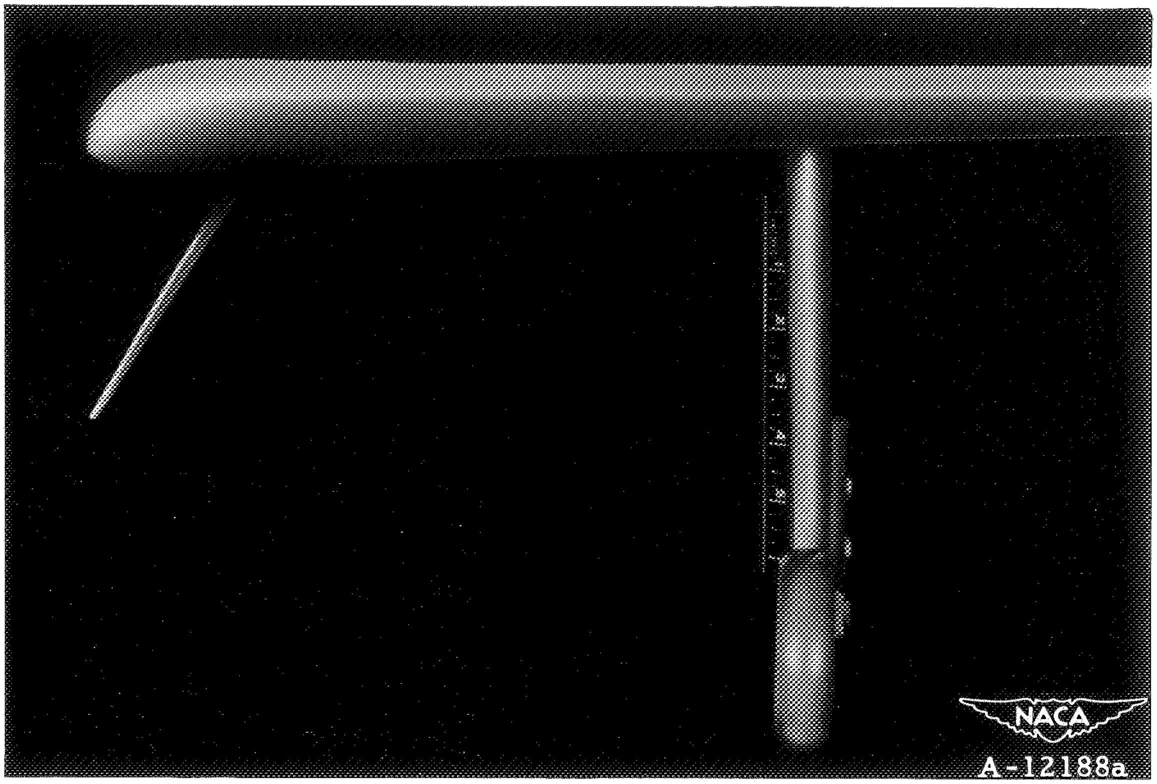

(a) Rear view.

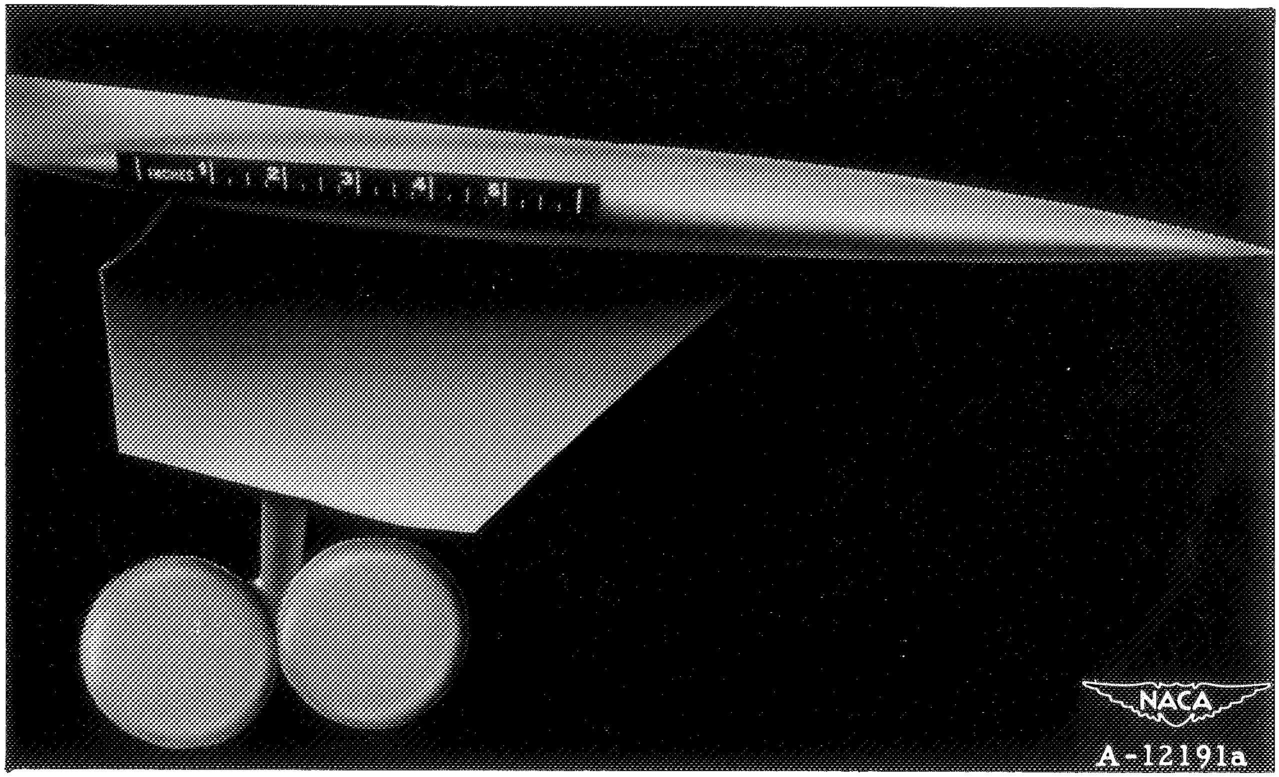

(b) Side view.

Figure 4.- Plain wing tip of the model with landing-gear door open.

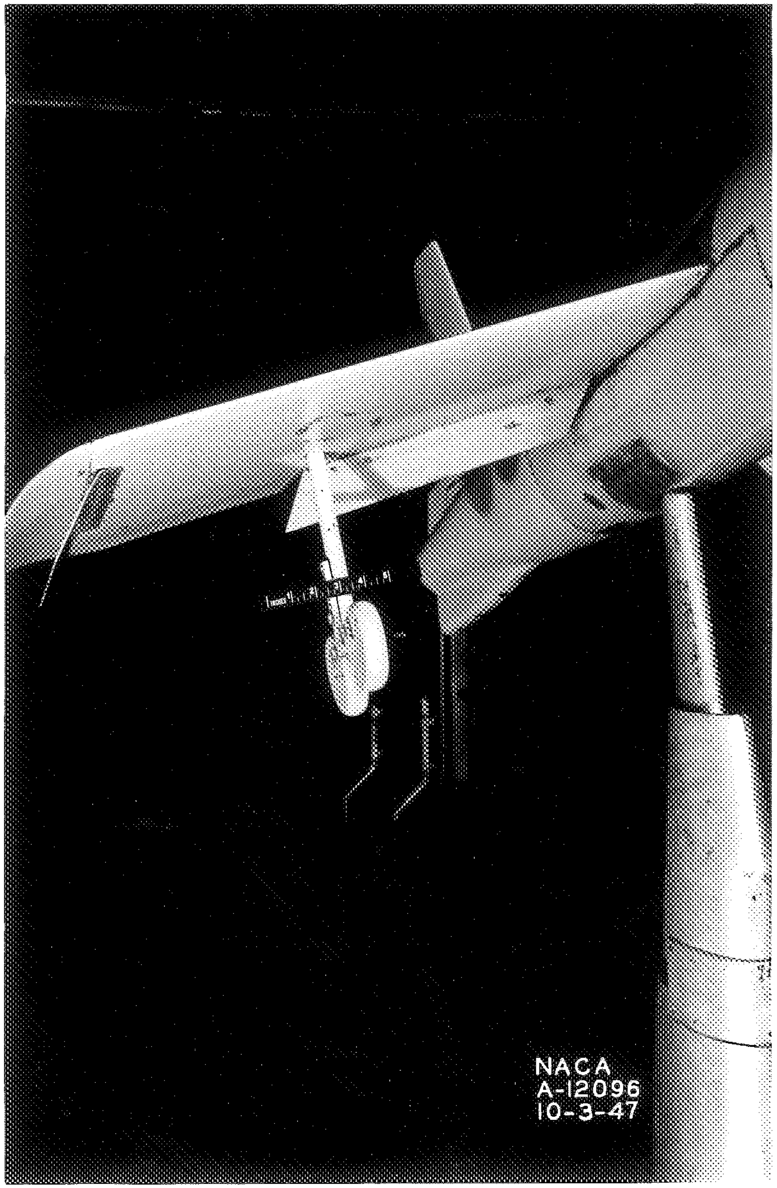

(a) Front view.

(b) Rear view.

Figure 5.- Drooped wing tip of the model with landing-gear door open.

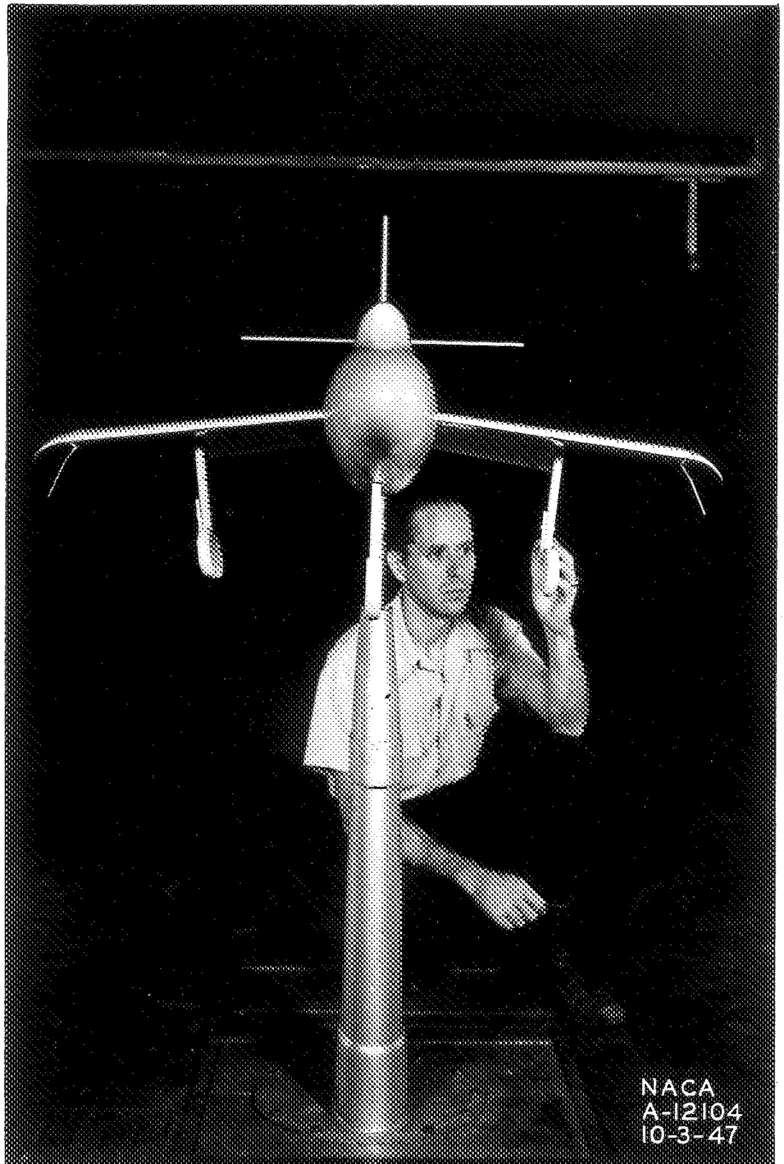

(a) Front view.

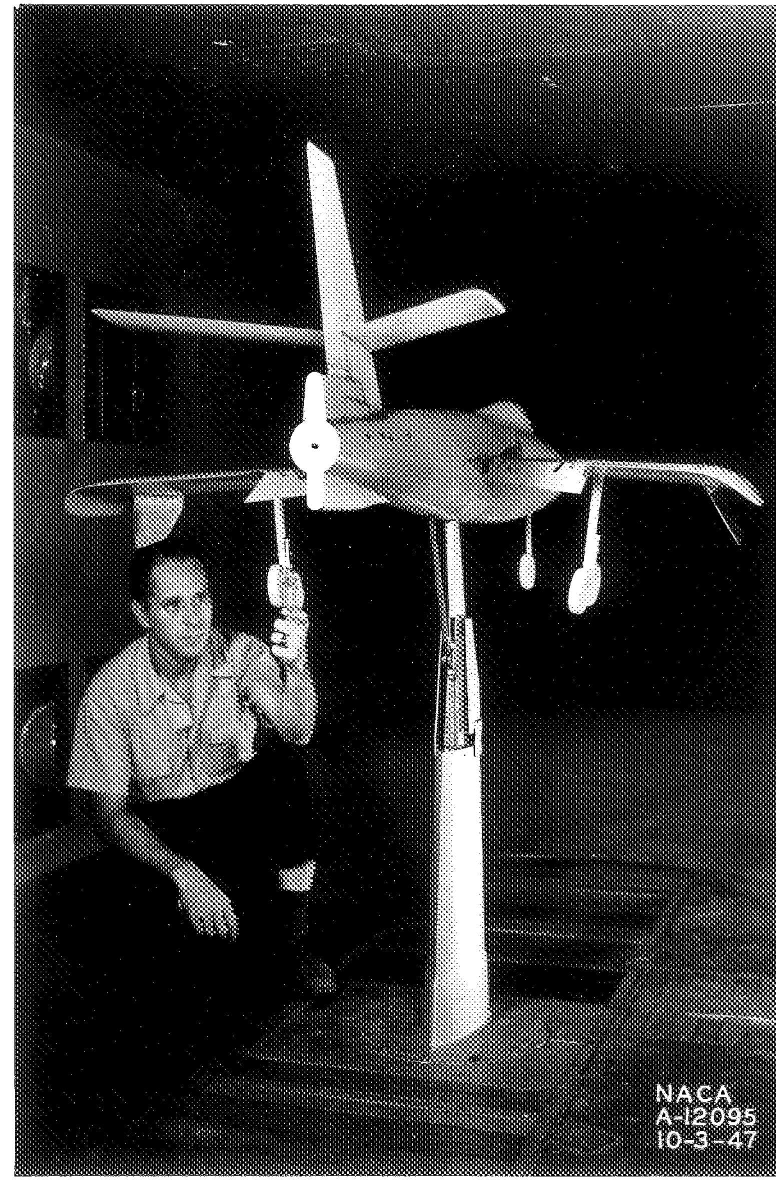

(b) Rear view.

Figure 6.- The 1/8-scale model of the Republic XP-91 airplane with conventional tail and drooped wing tips, flaps and gear down, landing-gear doors open.

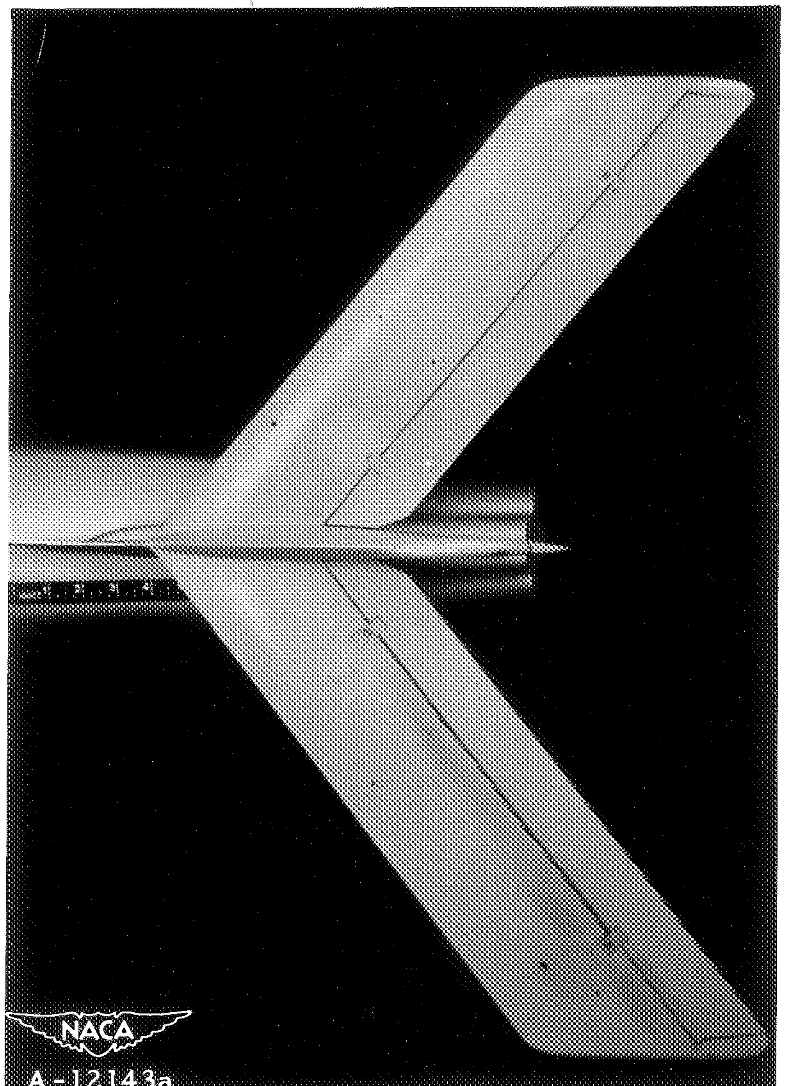

(a) Plan view.

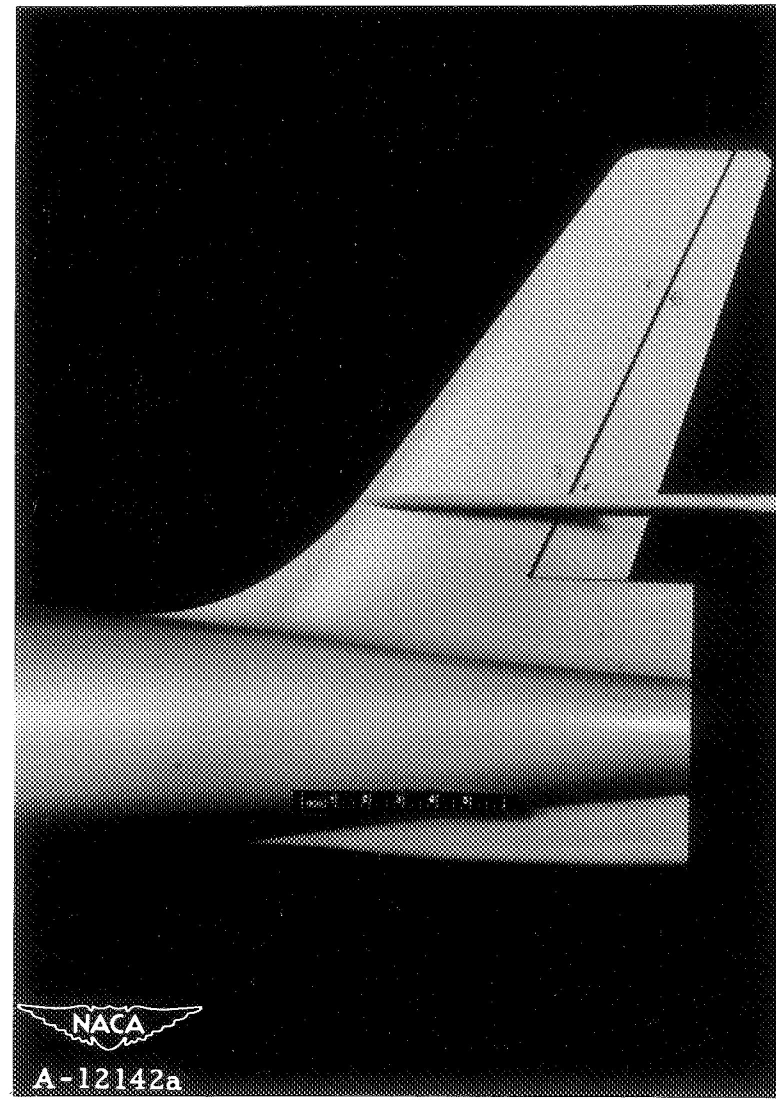

(b) Side view.

Figure 7.- The conventional tail.

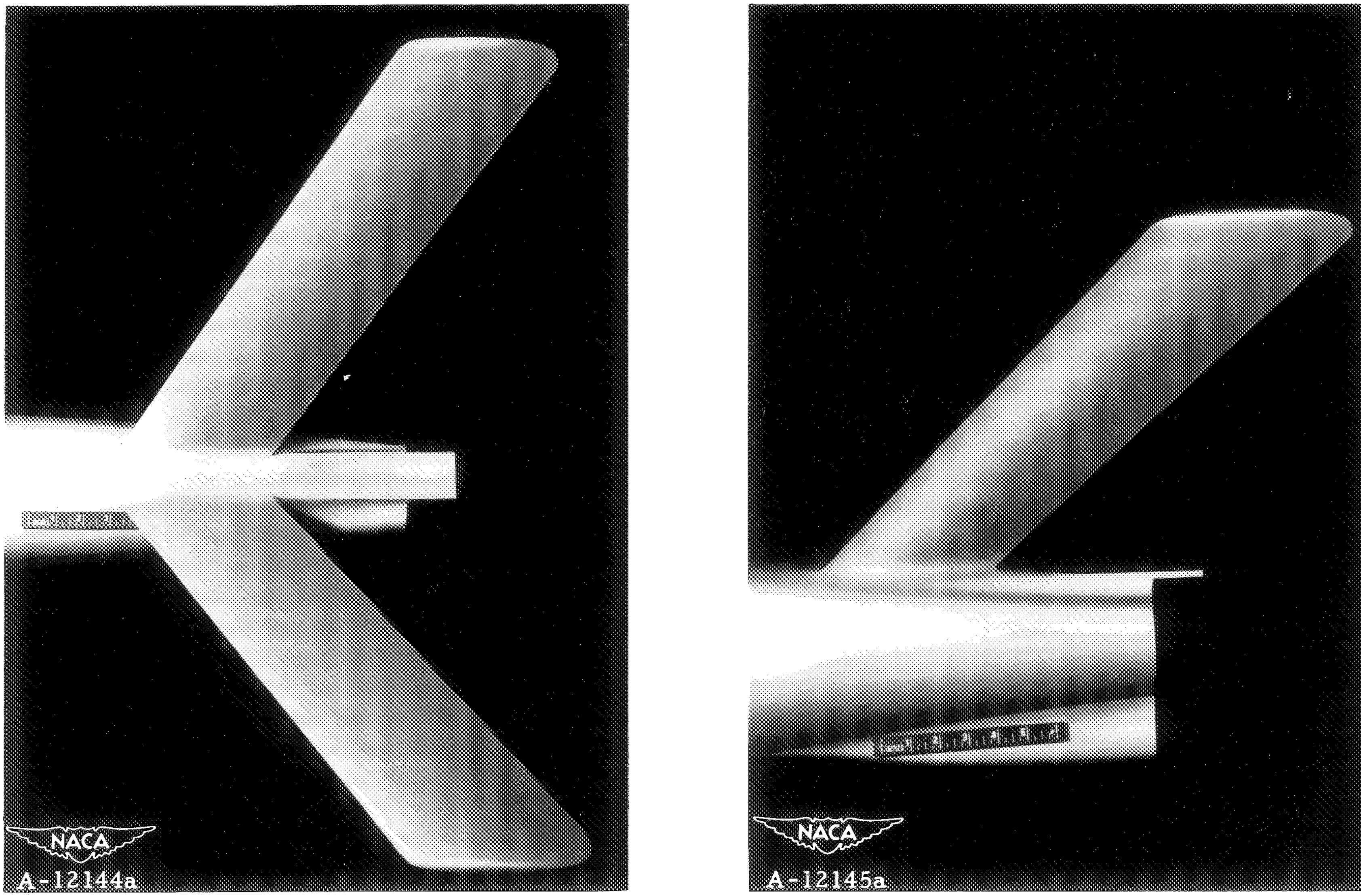

(a) Plan view.

(b) Side view.

Figure 8.- The vee tail in the forward position.

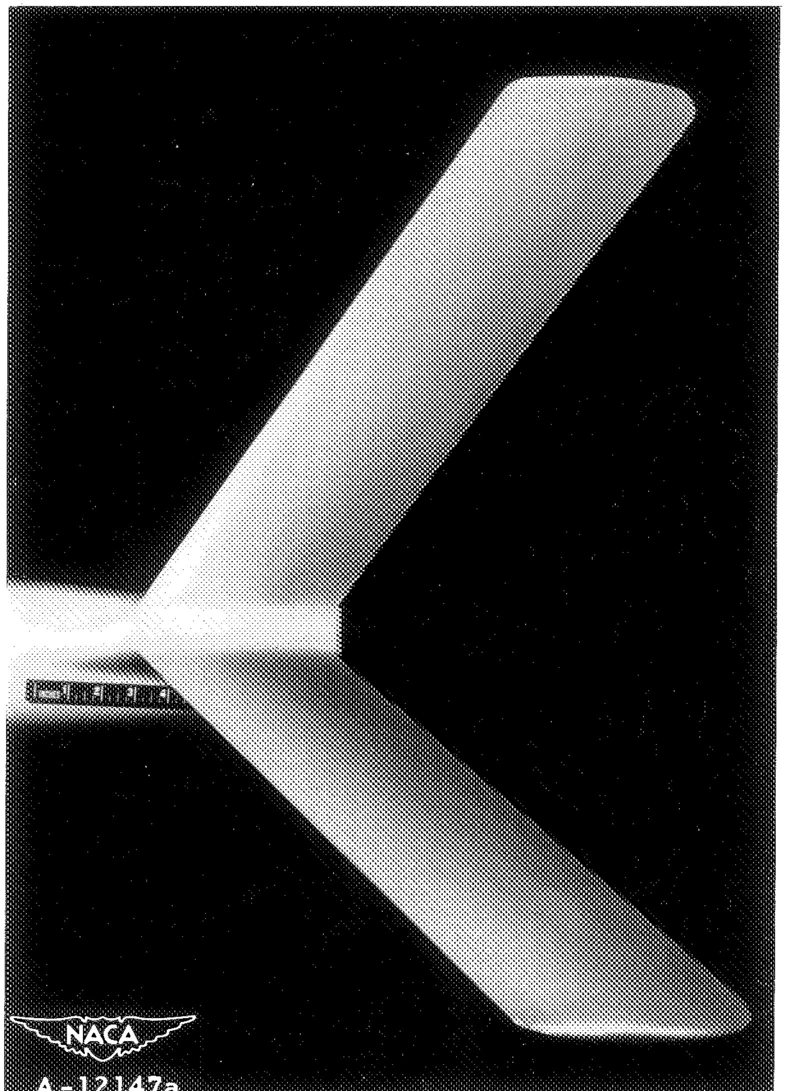

(a) Plan view.

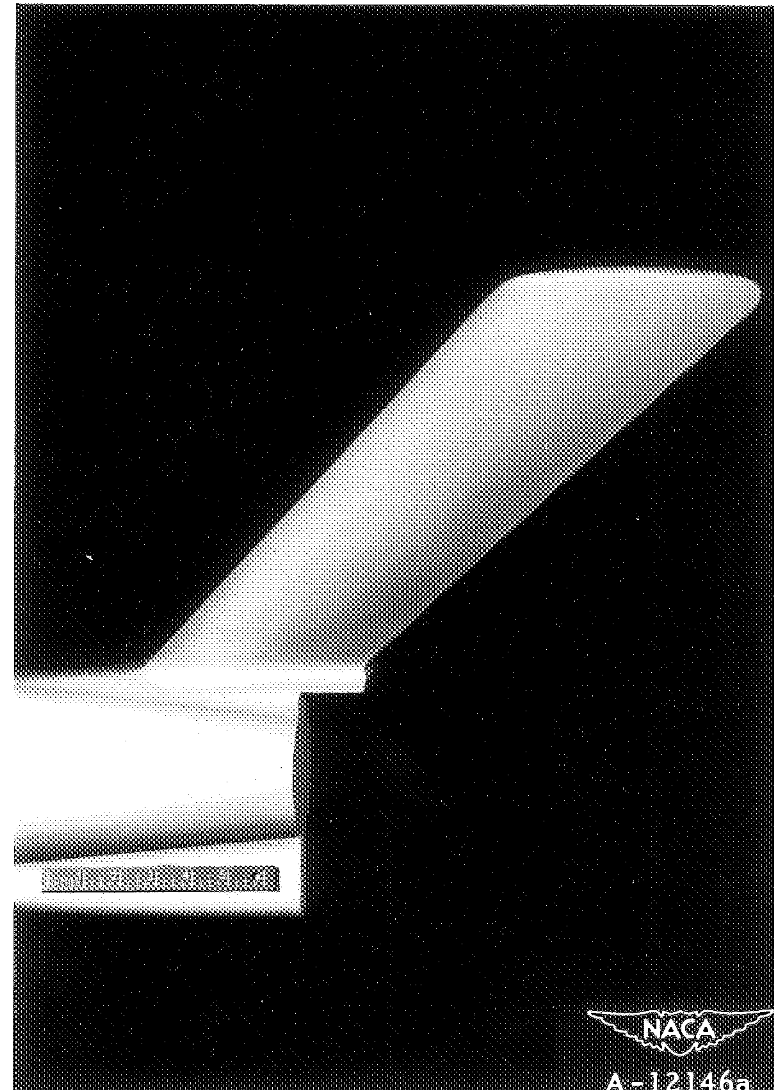

(b) Side view.

Figure 9.- The vee tail in the aft position.

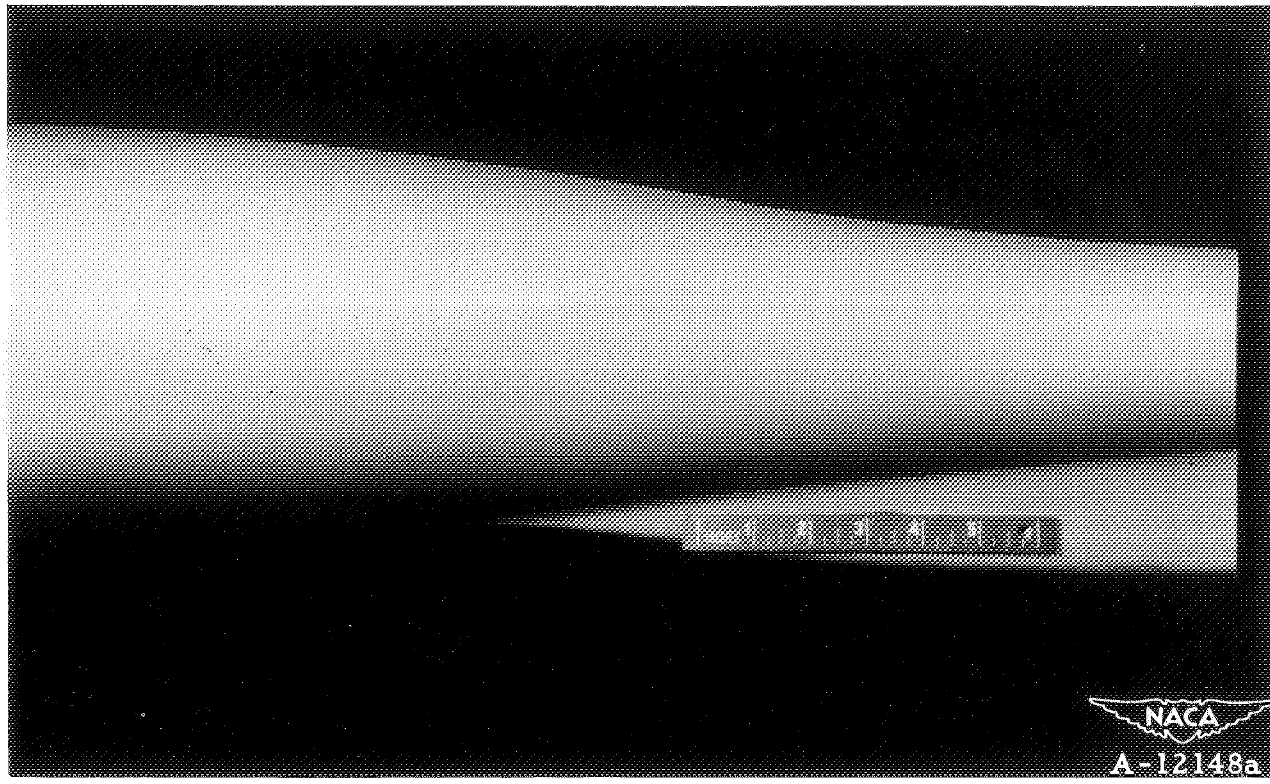

(a) Lower rocket fairing on.

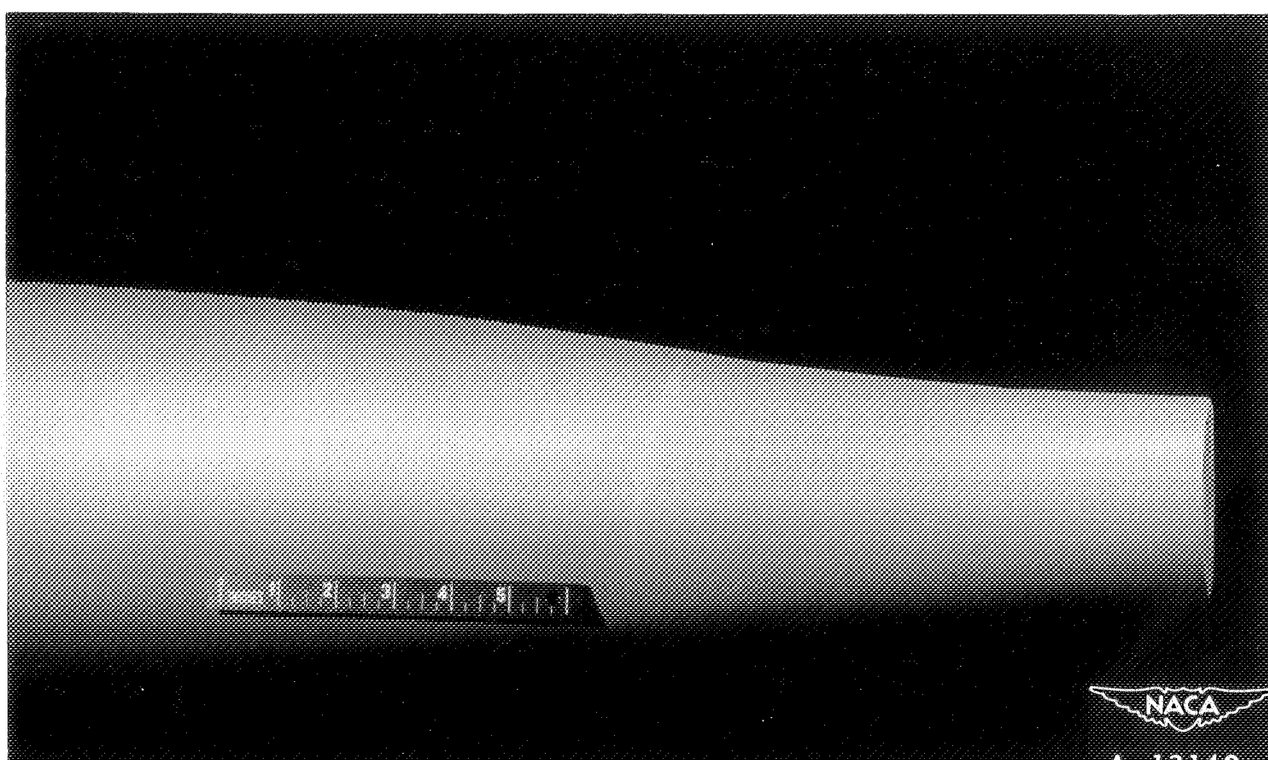

(b) Lower rocket fairing off.

Figure 10.- Rear portion of the fuselage with tail removed.

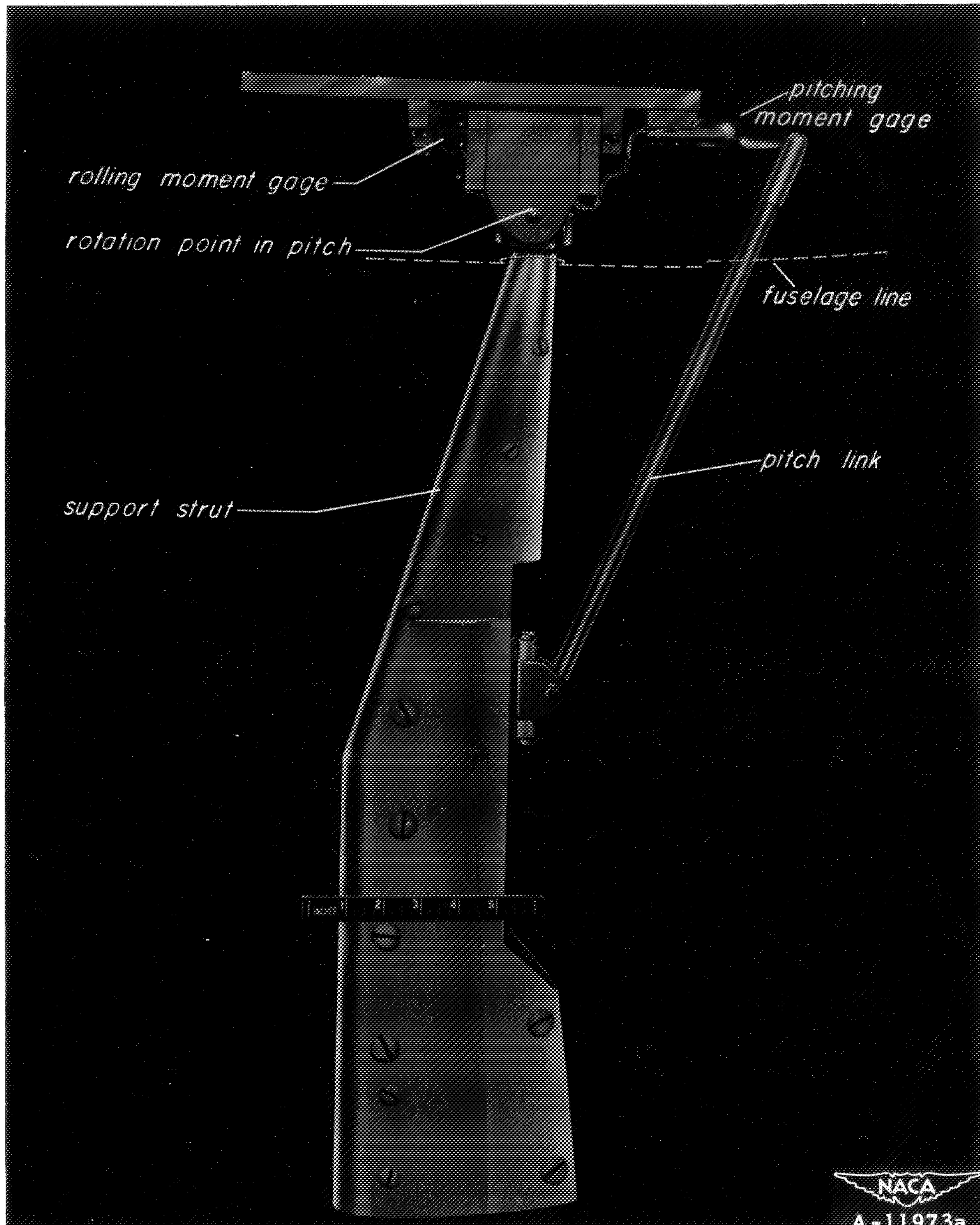

Figure 11.- Model support.

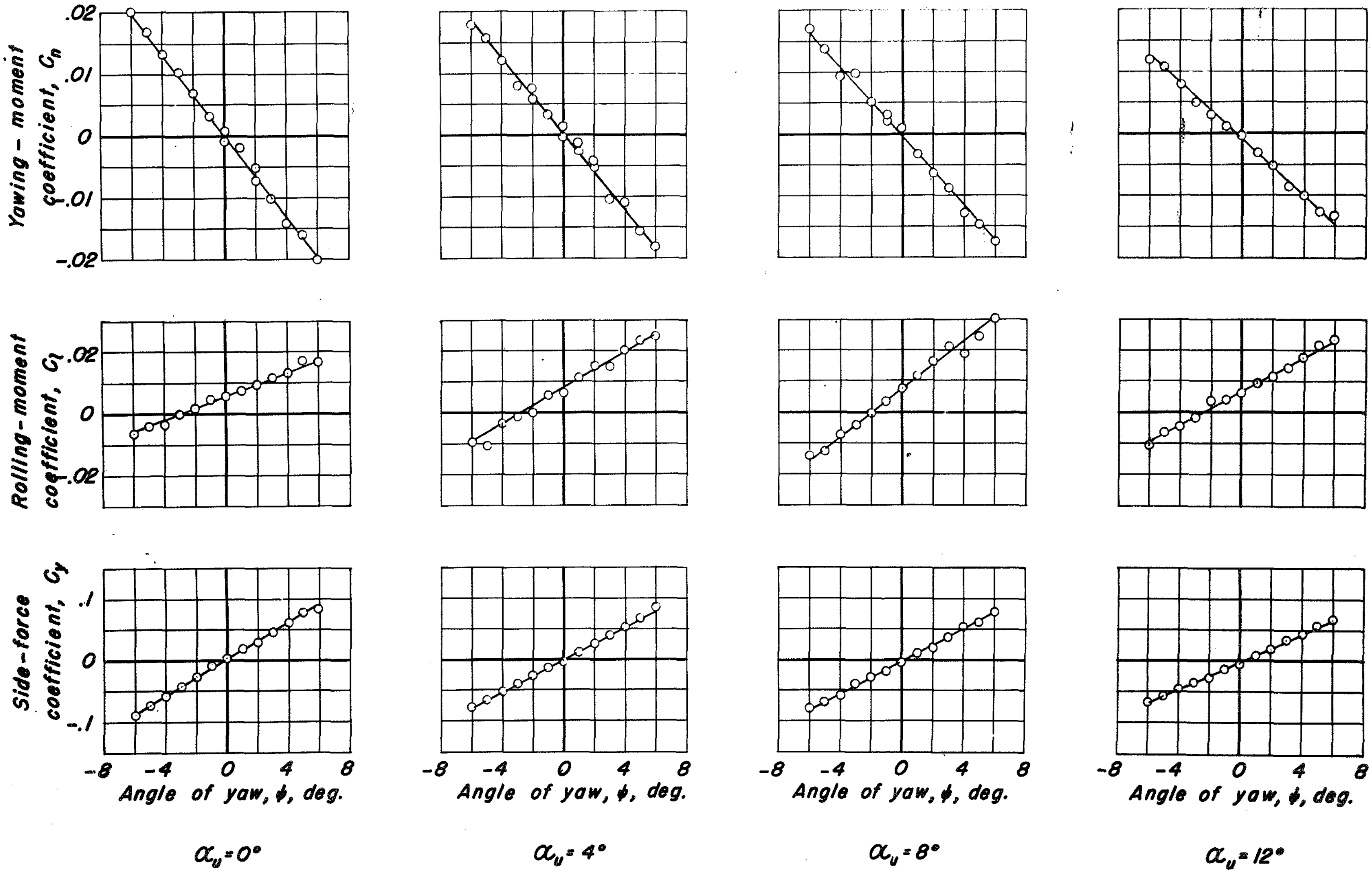

(a) Flaps up

Figure 12.- Lateral characteristics with conventional tail, plain wing tips.

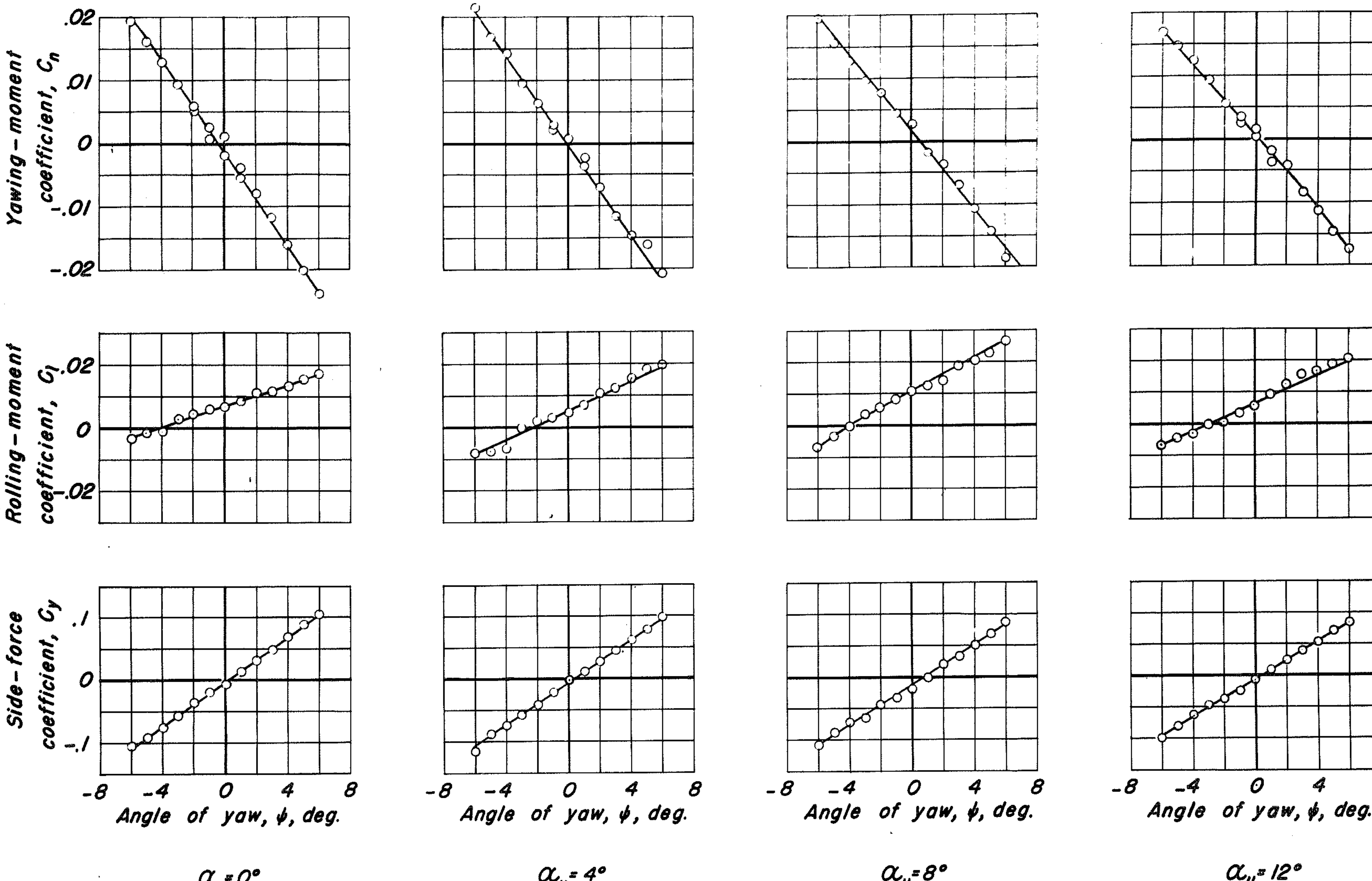

(b) Flaps and gear down, landing-gear doors open 125°.

Figure 12.- Concluded.

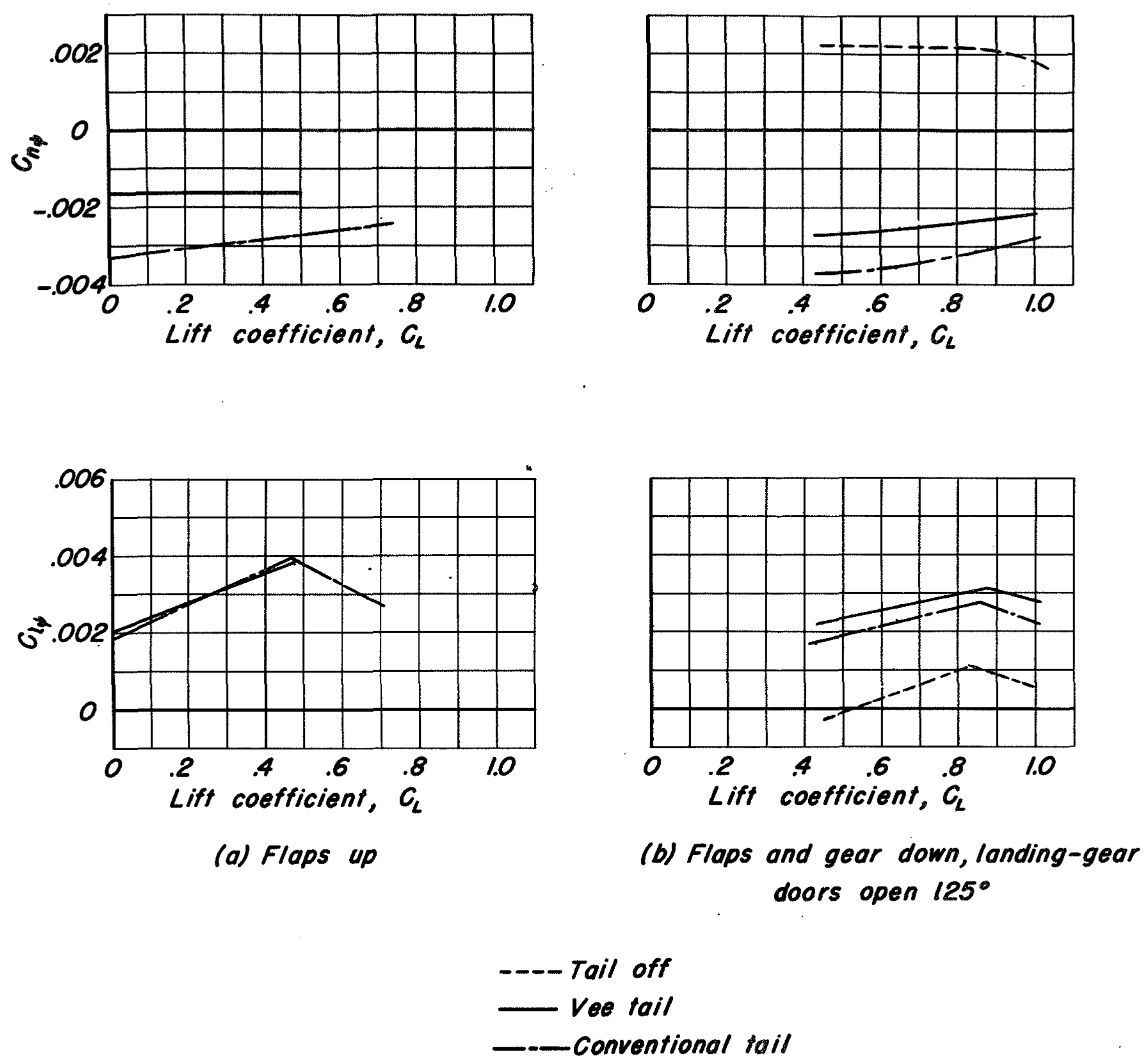

Figure 13.- Comparison of the lateral characteristics of the model with the vee and conventional tails, lower rocket fairing on, plain wing tips.

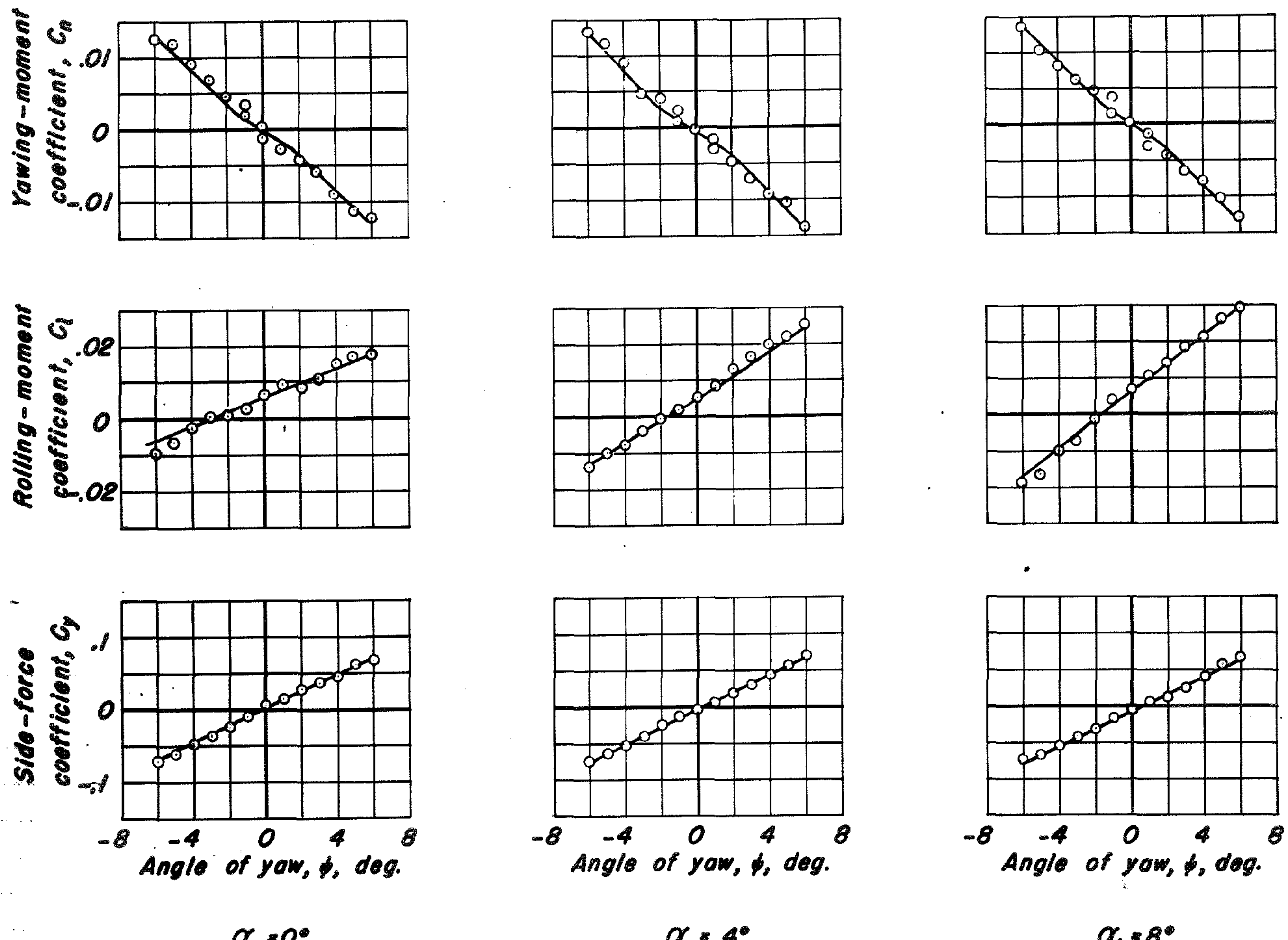

(a) Lower rocket fairing on.

Figure 14.- Lateral characteristics with vee tail, flaps up, plain wing tips.

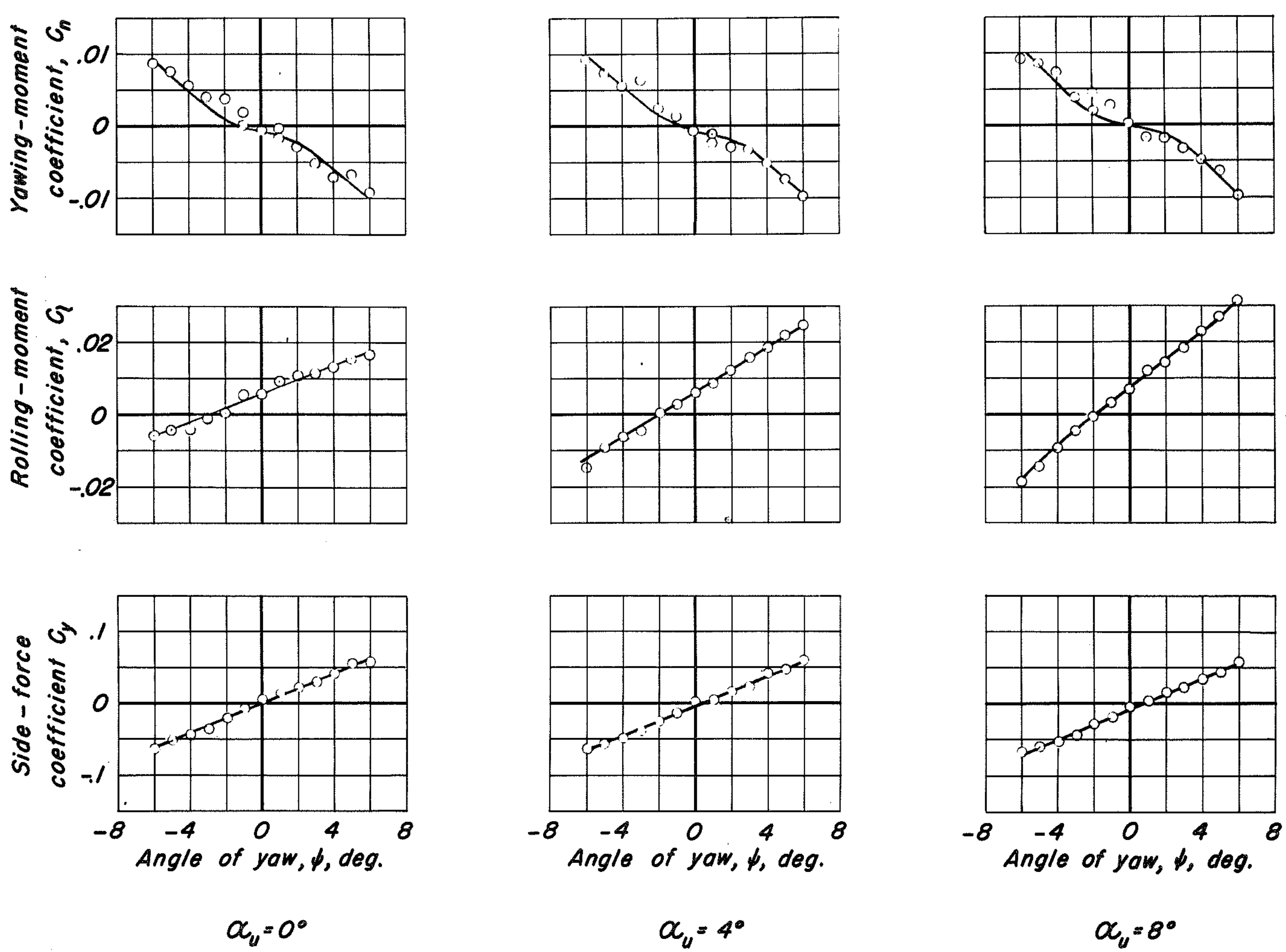

(b) Lower rocket fairing off.

Figure 14.- Concluded.

RM SA8A02

CONFIDENTIAL

NATIONAL ADVISORY COMMITTEE FOR AERONAUTICS

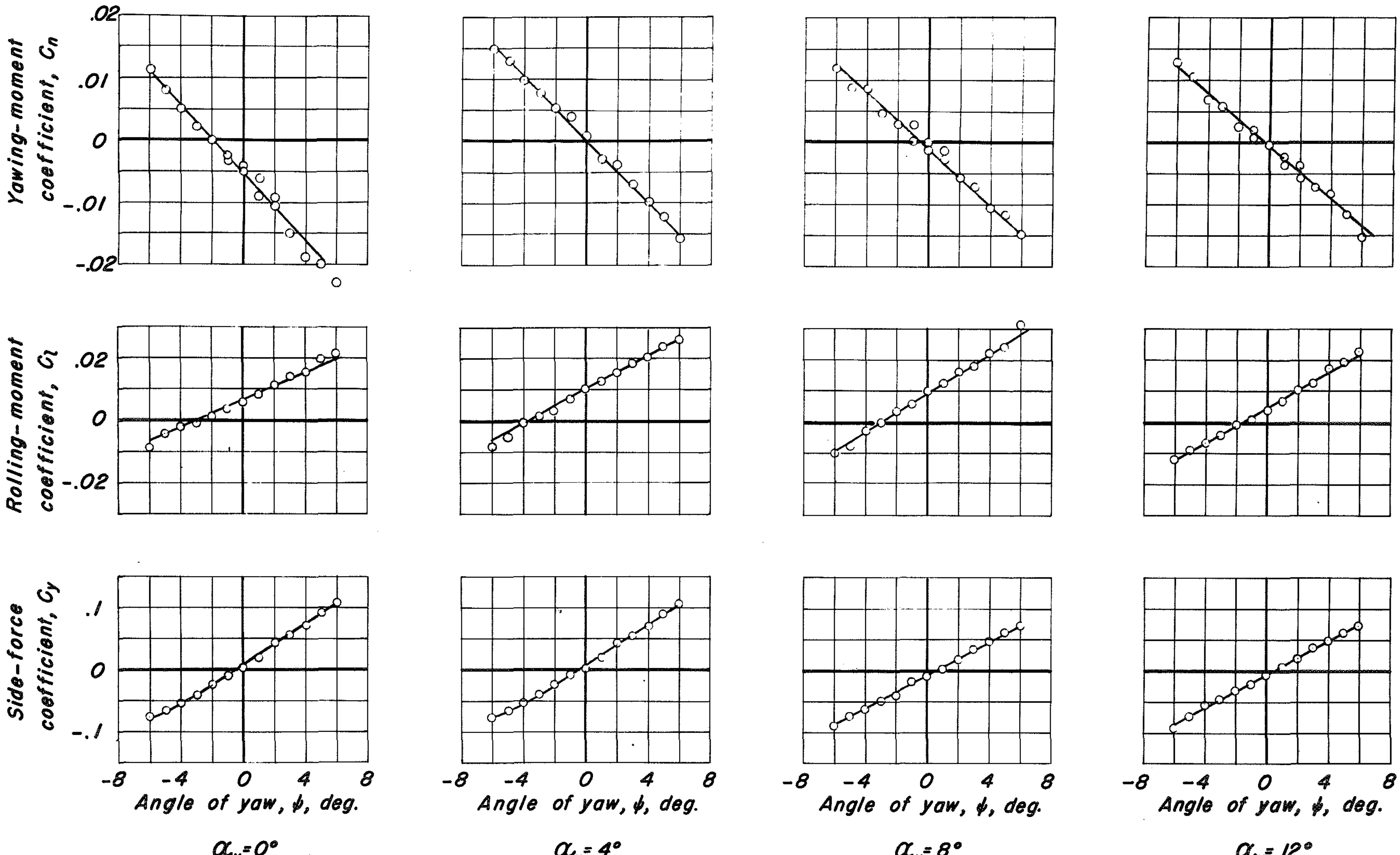

(a) Lower rocket fairing on.

Figure 15.- Lateral characteristics with the vee tail, flaps and gear down, landing-gear doors open 125°, plain wing tips.

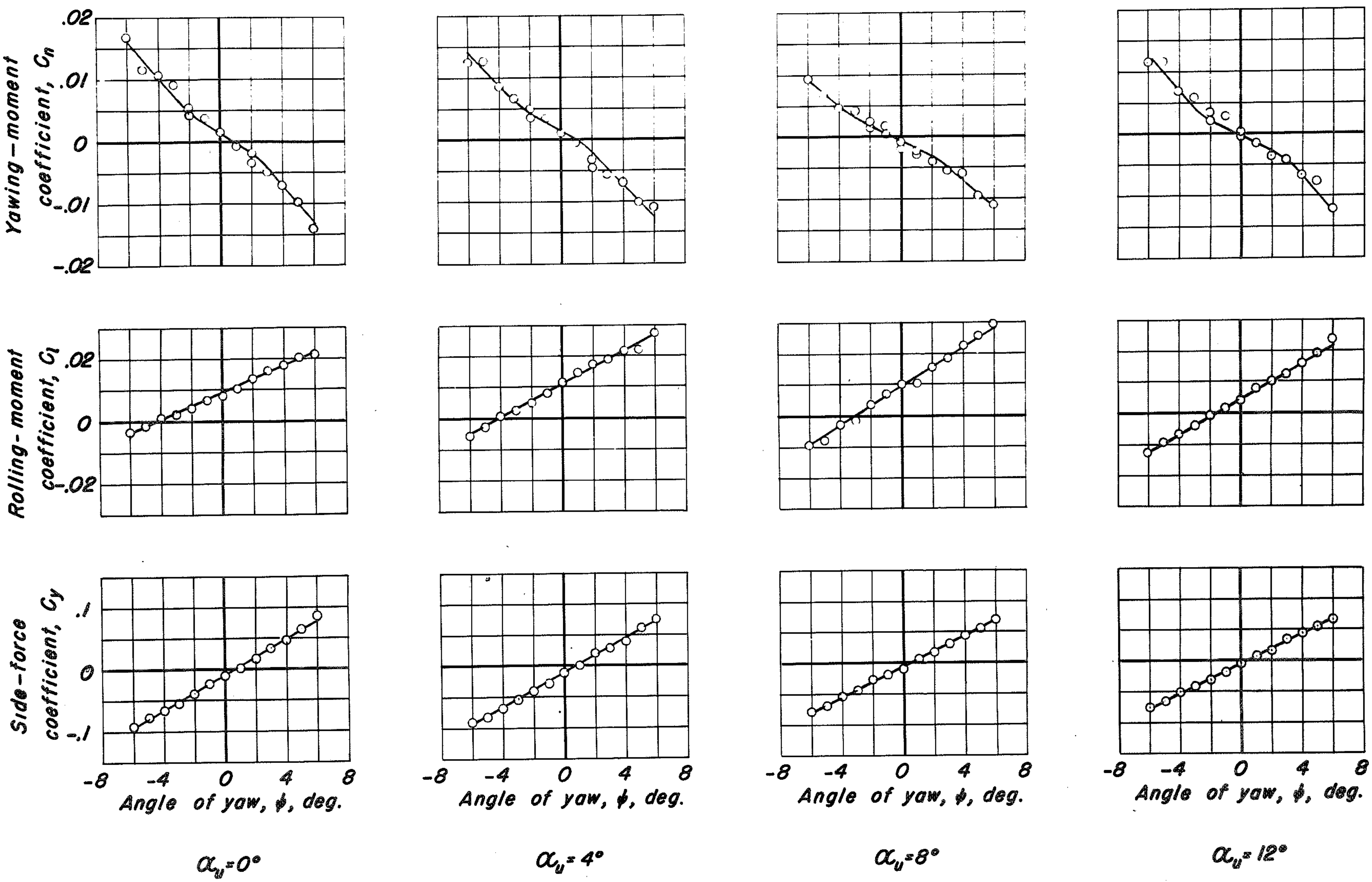

(b) Lower rocket fairing off.

Figure 15.- Concluded.

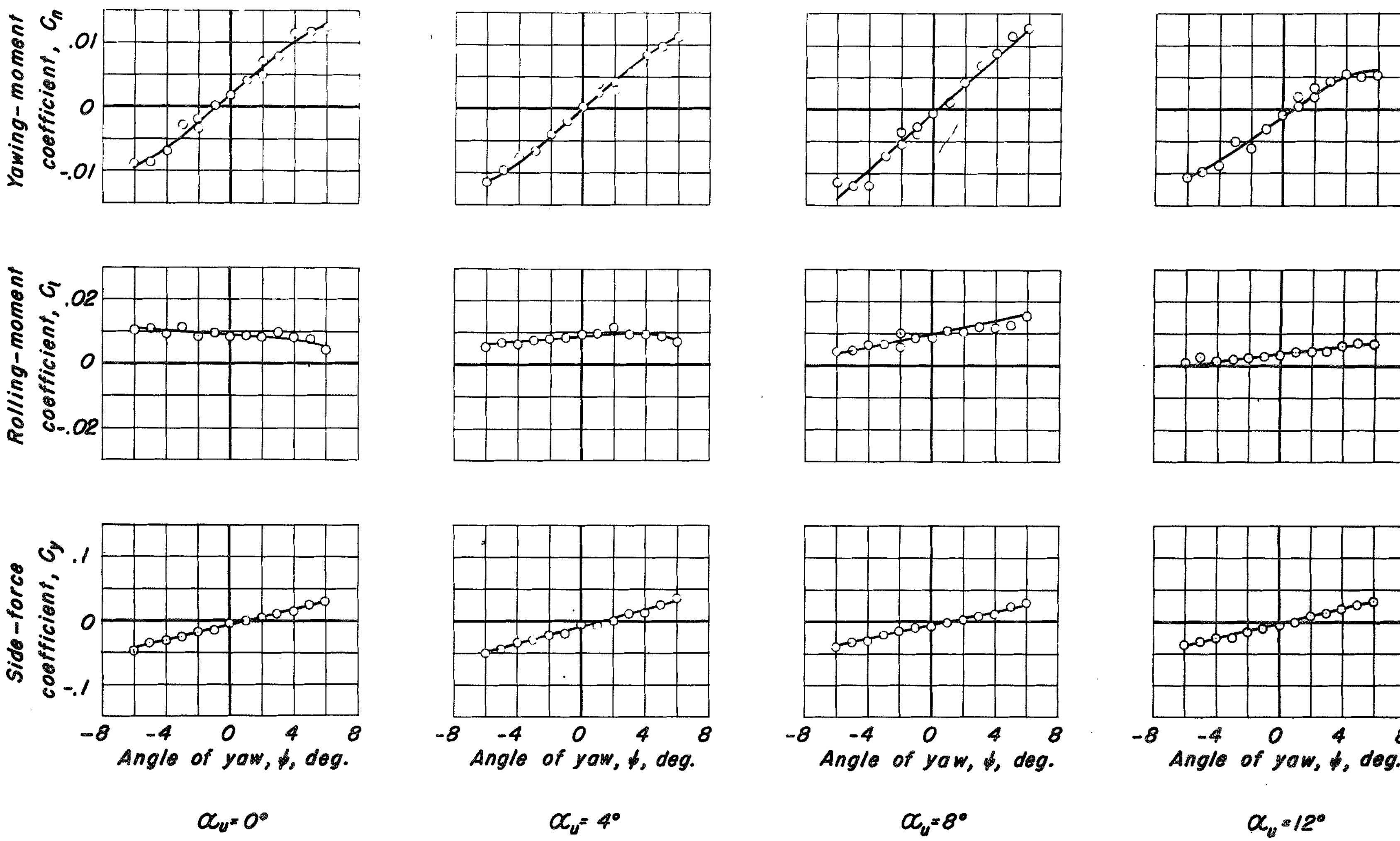

(a) Lower rocket fairing on.

Figure 16.- Lateral characteristics with tail off, flaps and gear down, landing-gear doors open 125°, plain wing tips.

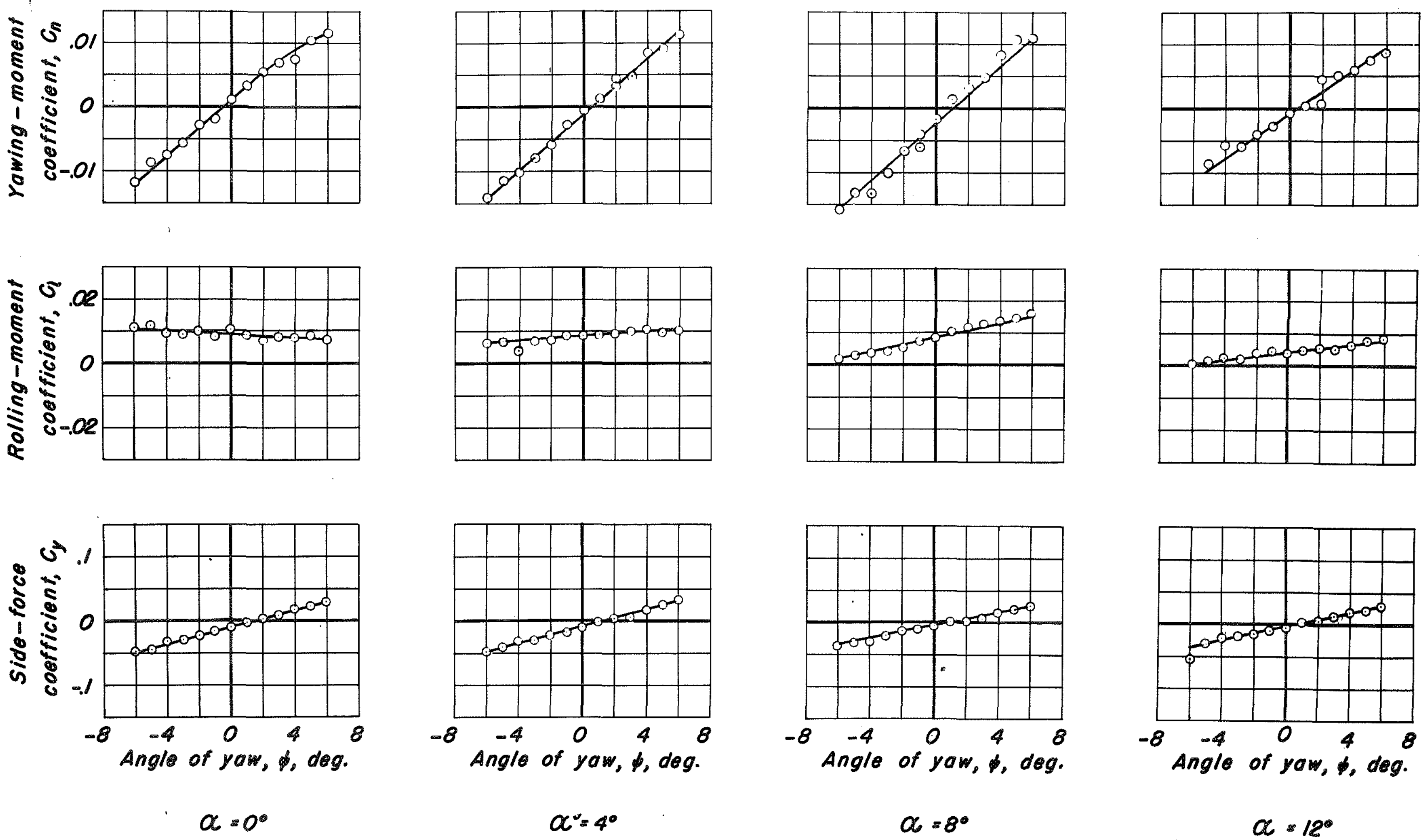

(b) Lower rocket fairing off.

Figure 16.- Concluded.

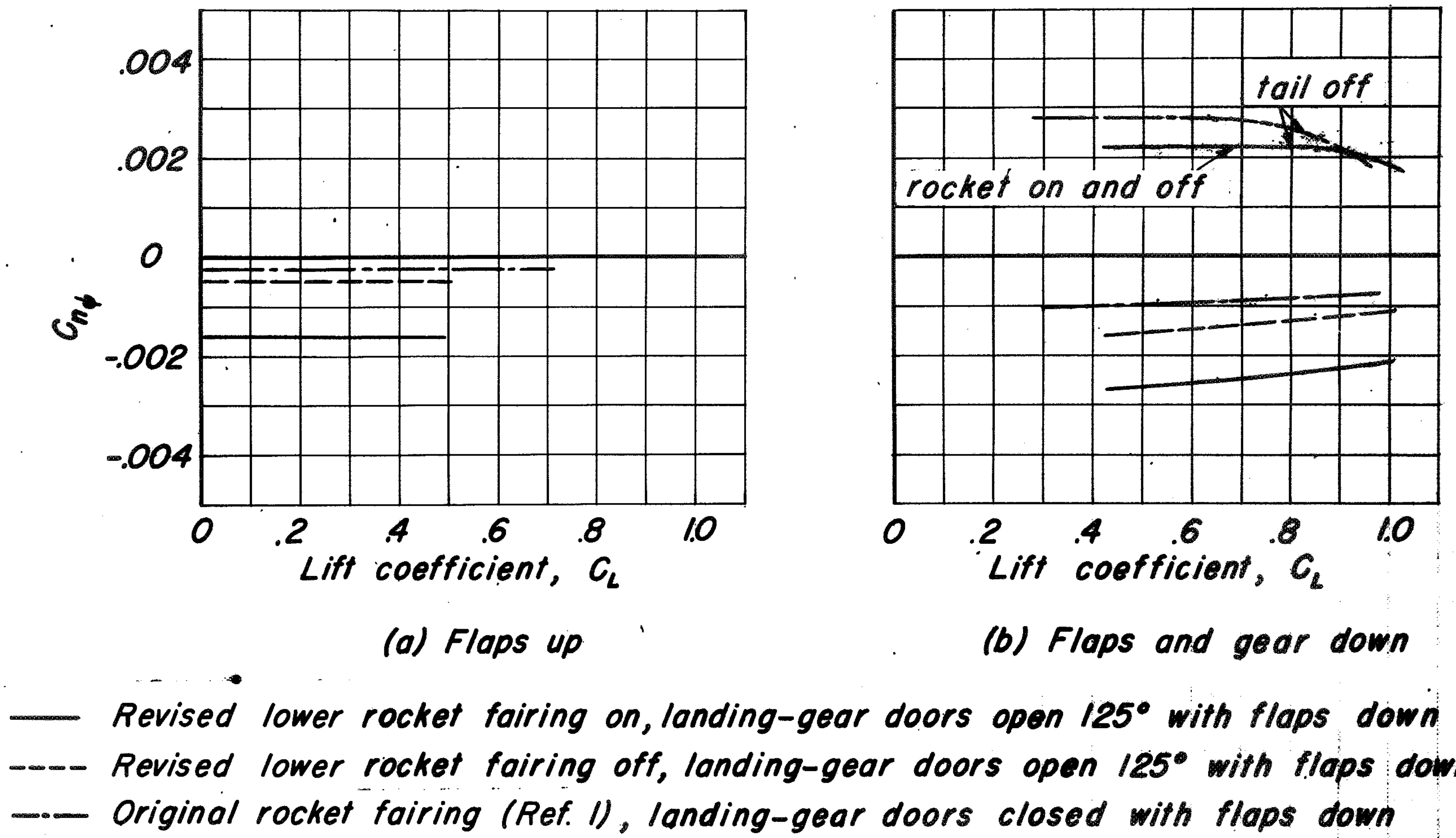

Figure 17.– Effect of rocket fairing on the variation of the parameter C_{n_ϕ} with lift coefficient, vee tail, plain wing tips.

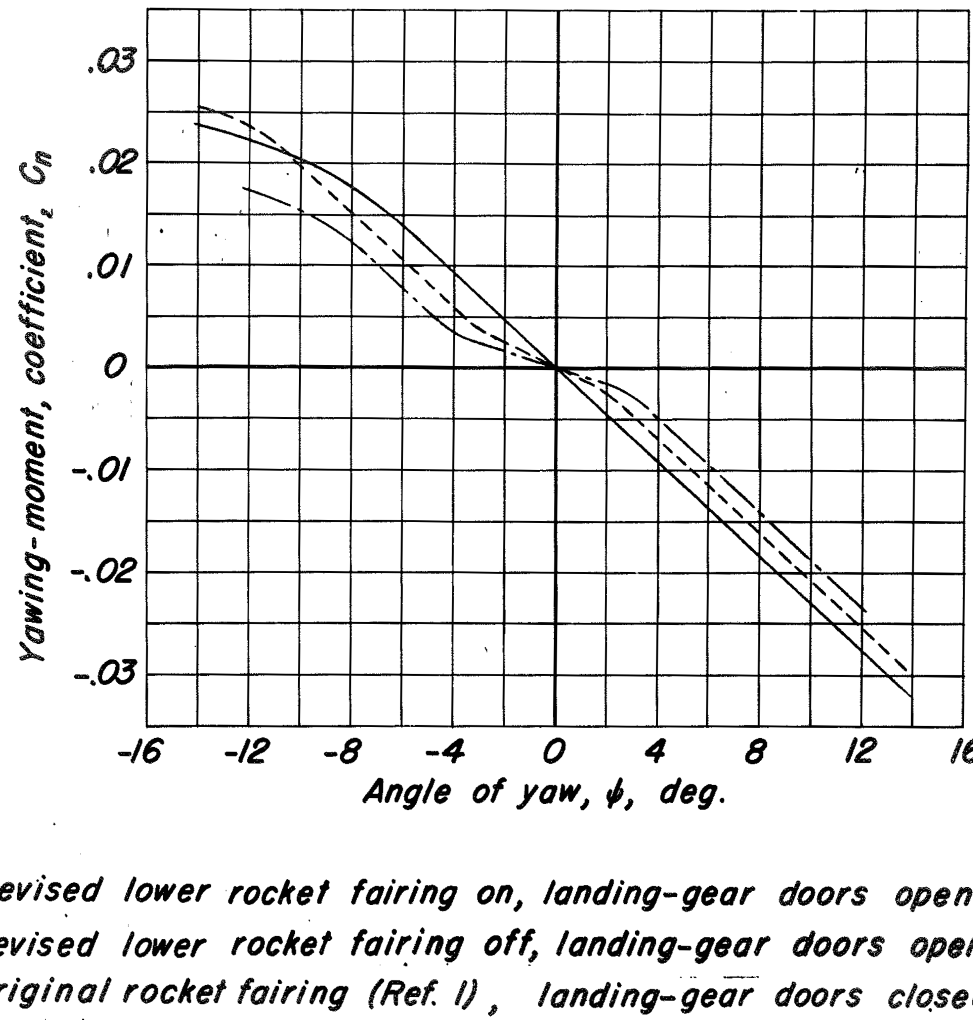

Figure 18.- Effect of rocket fairing on directional stability with the vee tail, flaps and gear down, plain wing tips, α_u=8°.

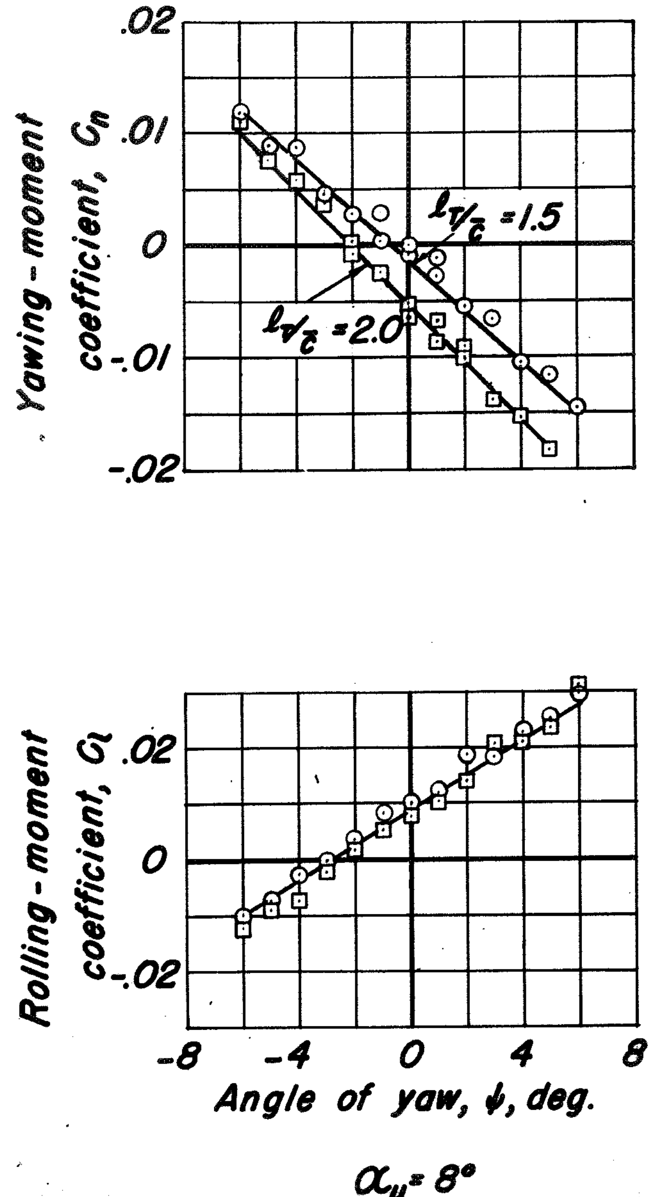

Figure 19.- Effect of tail length on lateral characteristics with vee tail, flaps and gear down, landing-gear doors open 125°, plain wing tips.

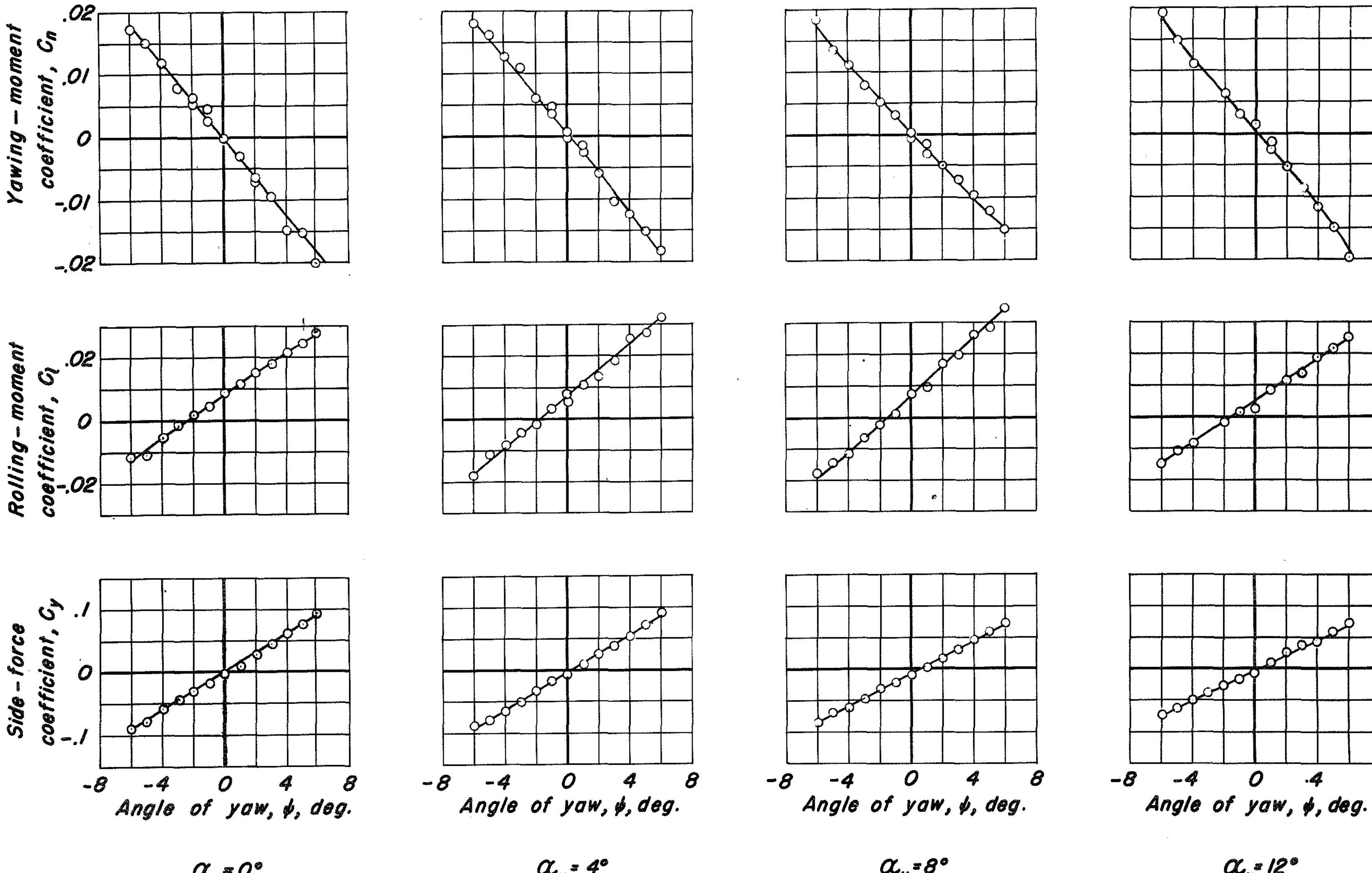

Figure 20.- Lateral characteristics with conventional tail, flaps and gear down, landing-gear doors closed, plain wing tips.

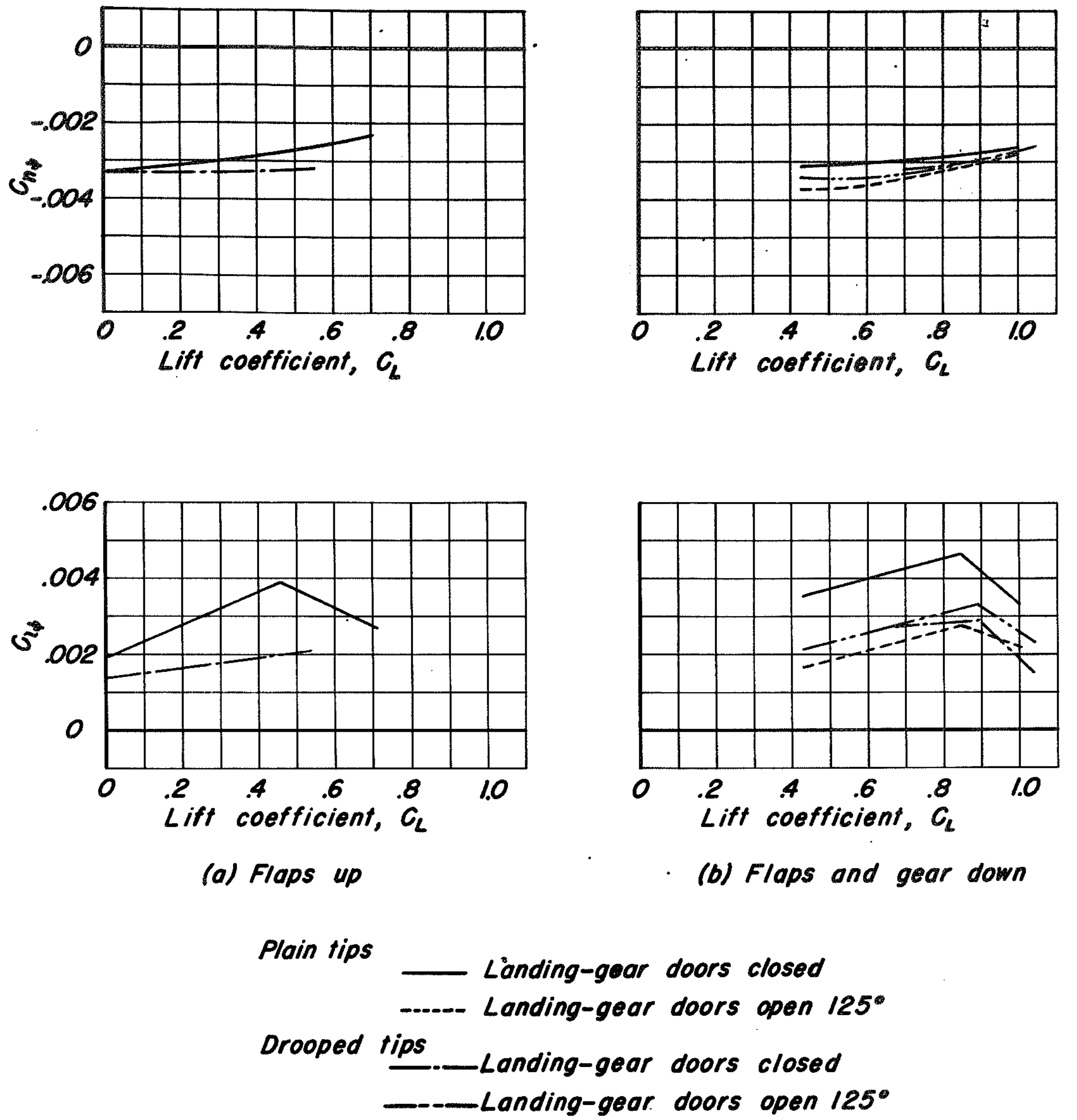

Figure 21.- Effect of drooped wing tips and landing-gear doors on the variation of the parameters C_{l_ψ} and C_{n_ψ} with lift coefficient.

RM SA8A02

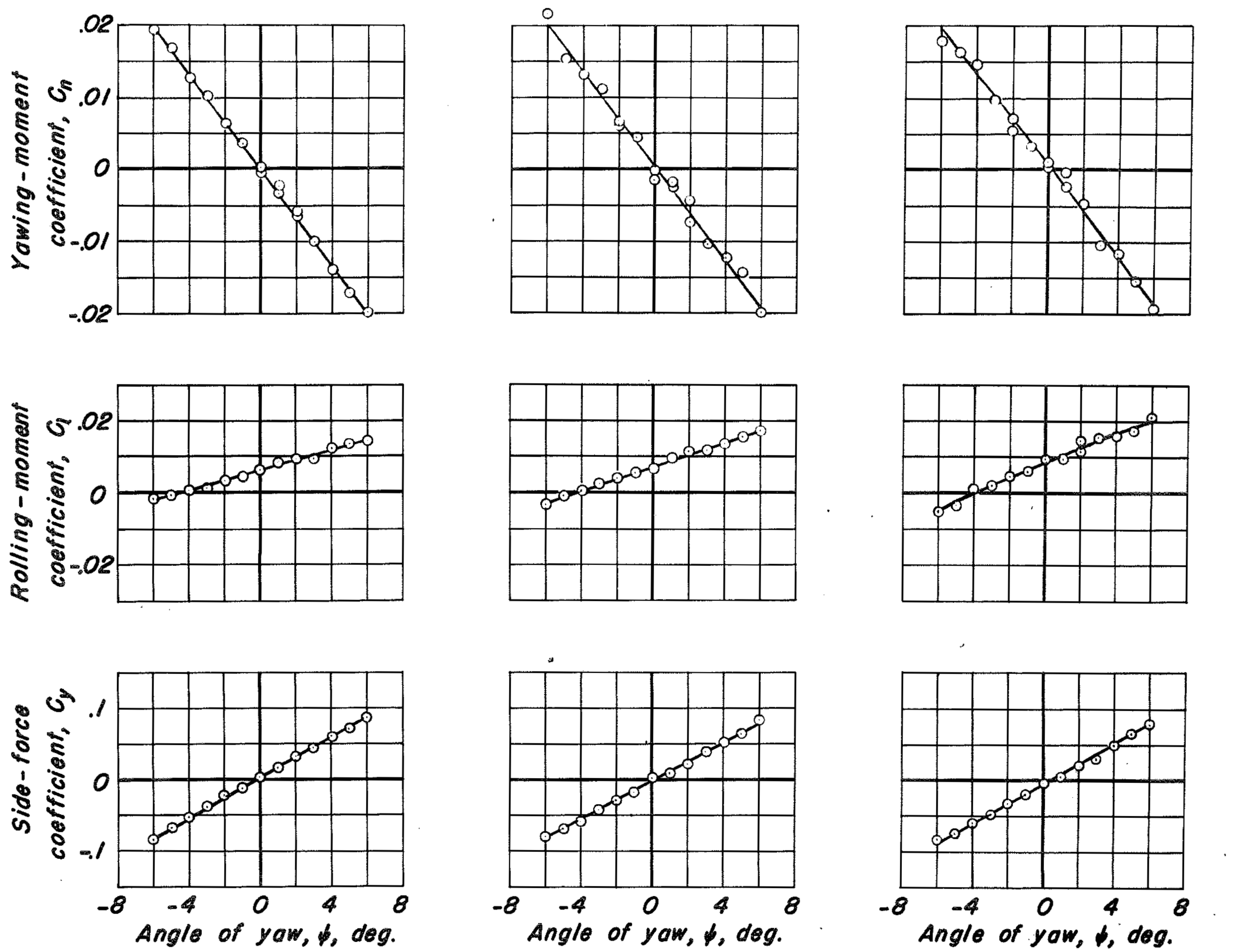

$\alpha_u = 0°$ $\alpha_u = 4°$ $\alpha_u = 8°$

(a) Flaps up.

Figure 22.- Lateral characteristics with conventional tail, drooped wing tips.

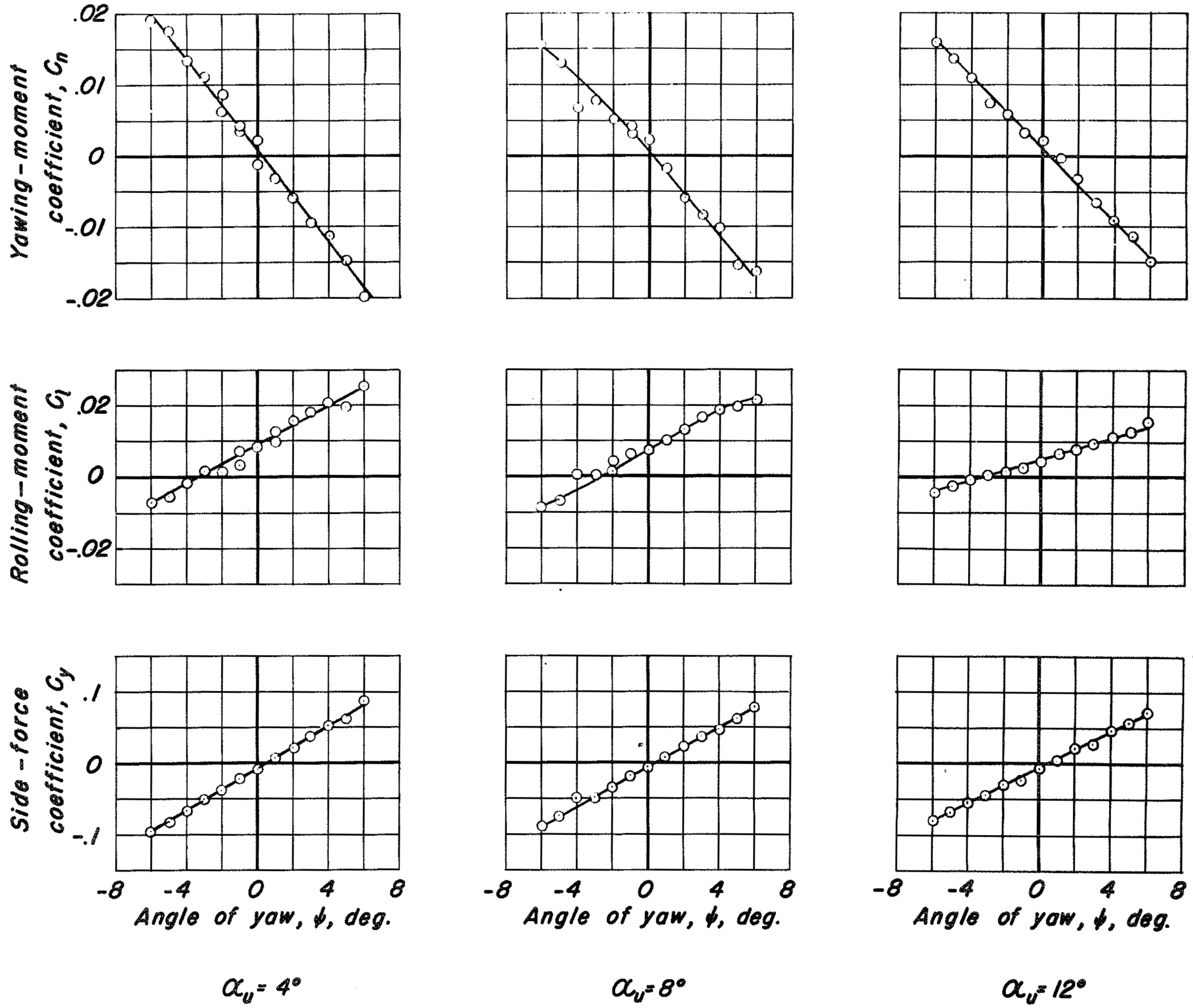

(b) Flaps and gear down, landing-gear doors closed.

Figure 22.- Continued.

NACA RM SA8A02

CONFIDENTIAL

NATIONAL ADVISORY COMMITTEE FOR AERONAUTICS

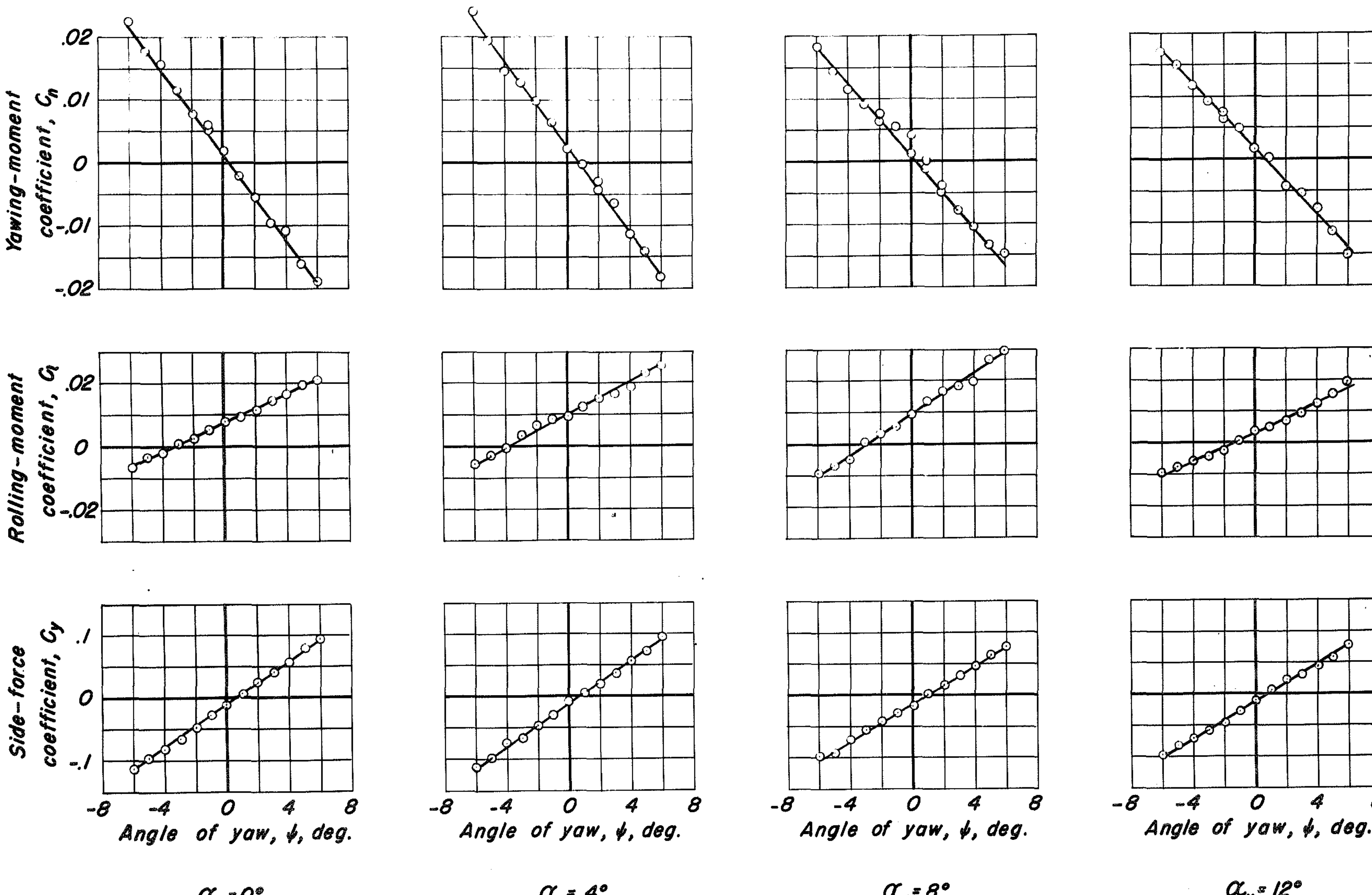

(c) Flaps and gear down, landing-gear doors open 125°.

Figure 22.- Concluded.

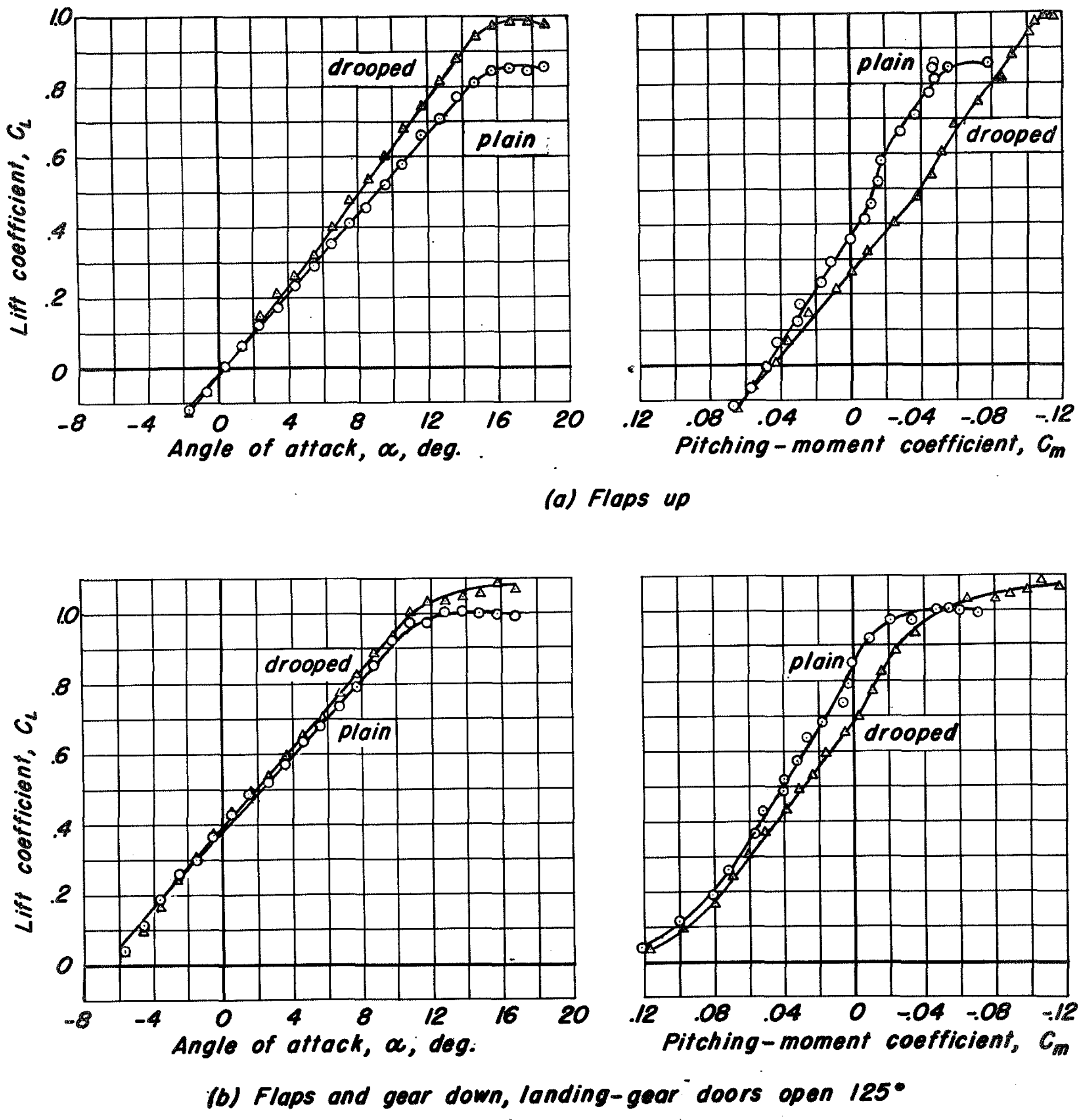

Figure 23.- Effect of drooped wing tips on the longitudinal characteristics with the conventional tail.

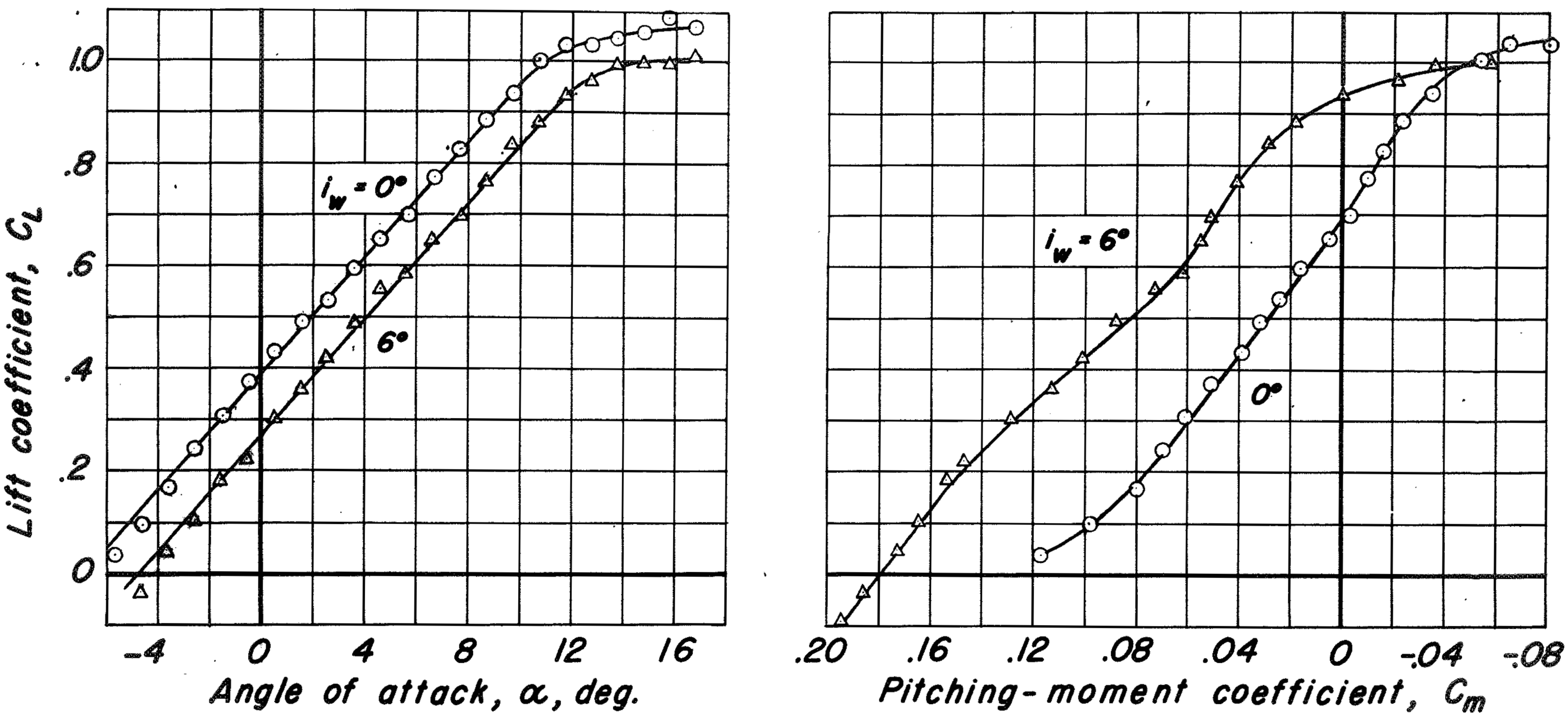

Figure 24.– Effect of 6° wing incidence on longitudinal characteristics with the conventional tail, flaps and gear down, landing-gear doors open 125°, drooped wing tips.

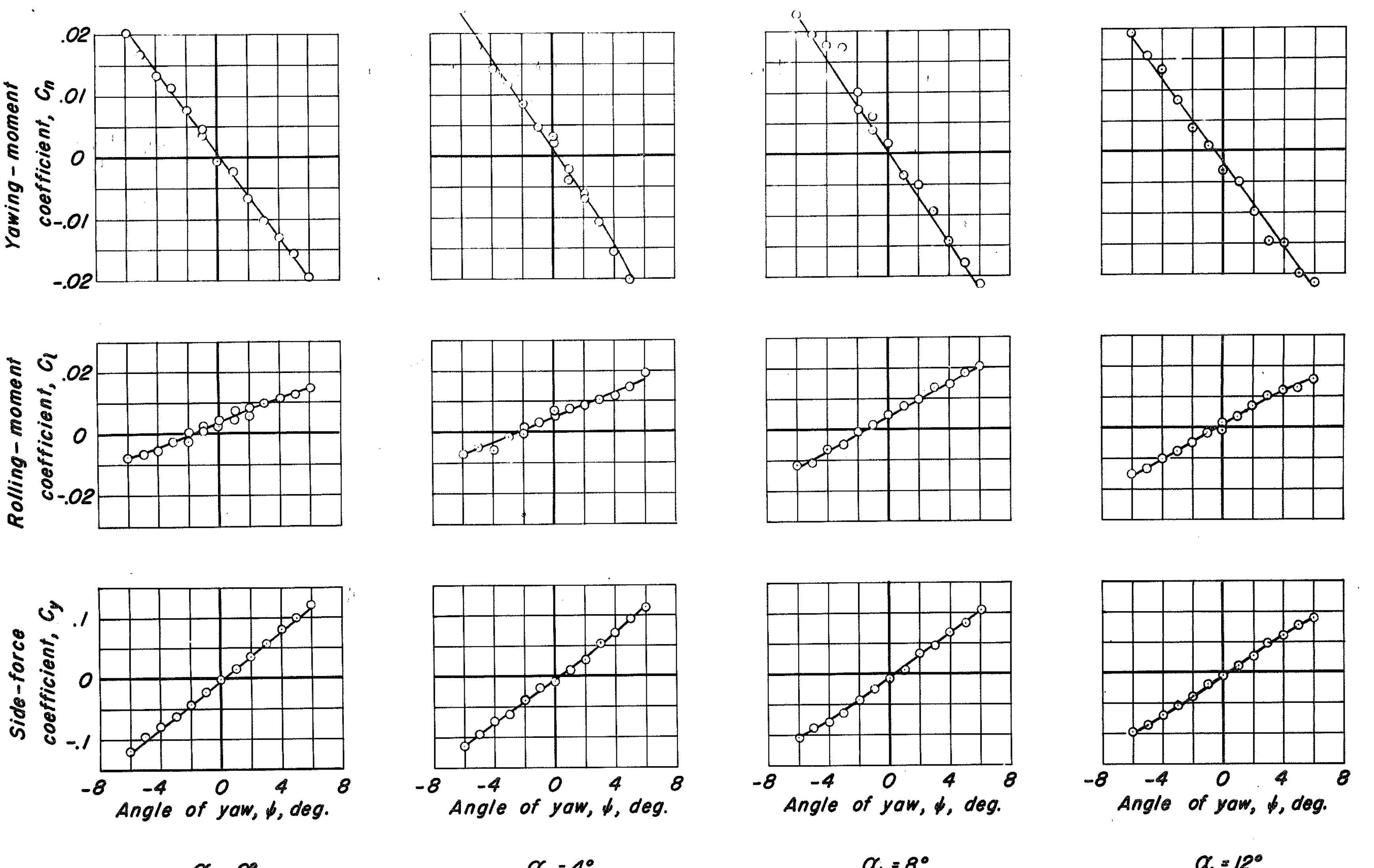

Figure 25.- Lateral characteristics with 6° wing incidence, conventional tail, flaps and gear down, landing-gear doors open 125°, plain wing tips.

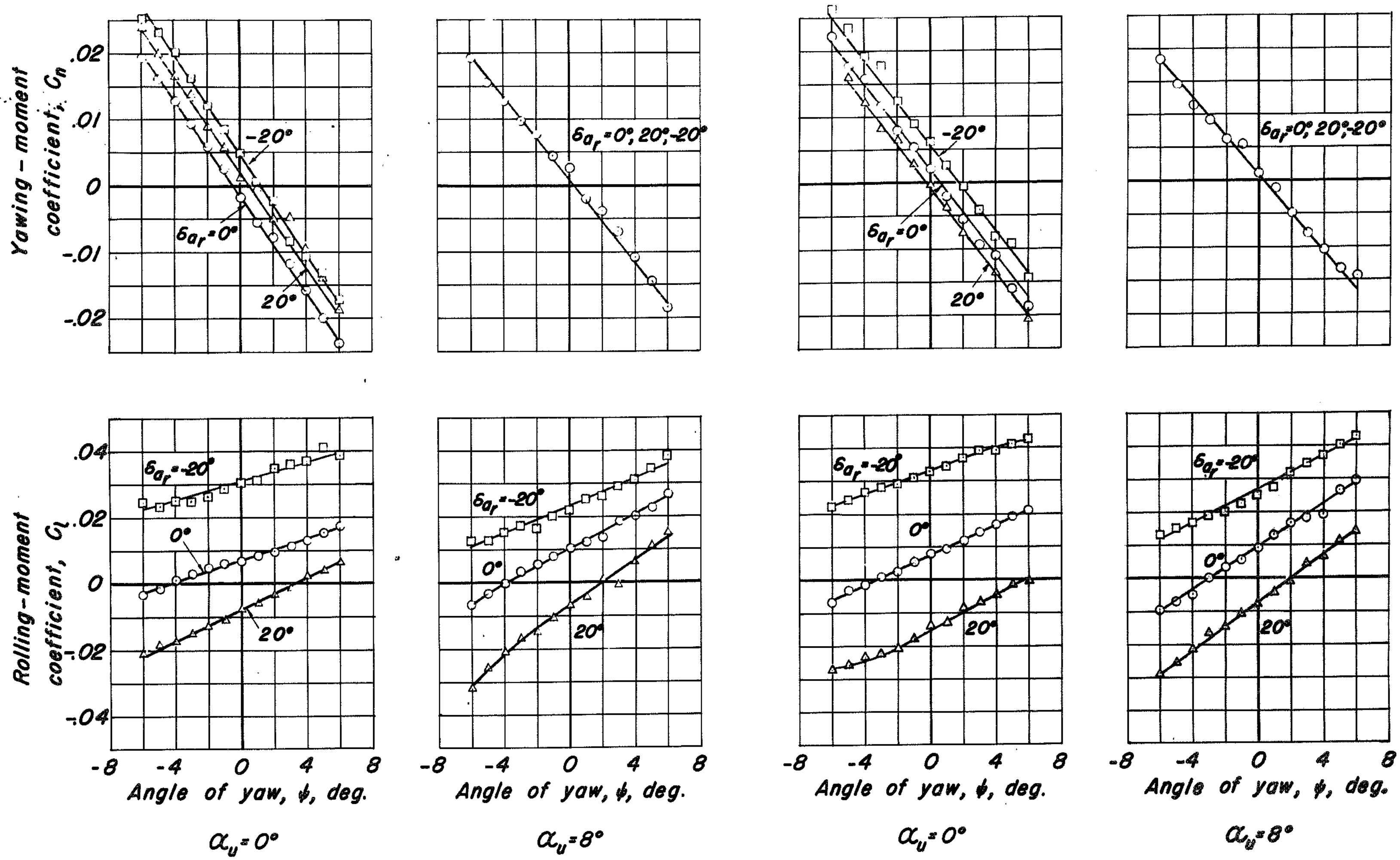

(a) Plain wing tips

(b) Drooped wing tips

Figure 26.- Aileron effectiveness with flaps and gear down, landing-gear doors open 125°, conventional tail.

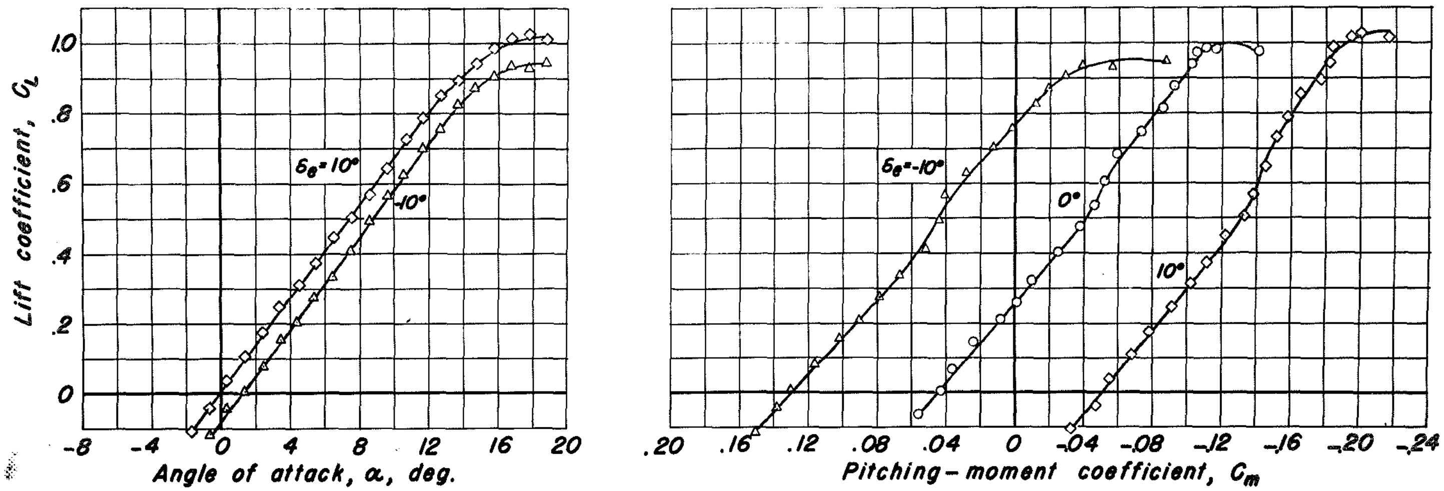

(a) Flaps up

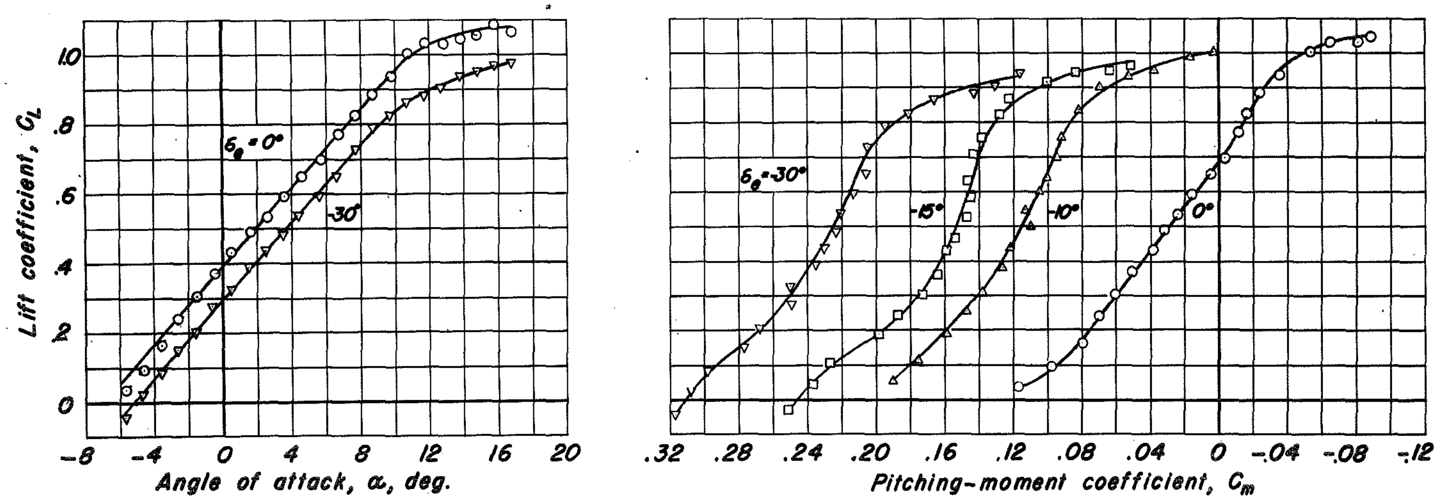

(b) Flaps and gear down, landing-gear doors open 125°

Figure 27.- Effectiveness of the elevators on the conventional tail, drooped wing tips.

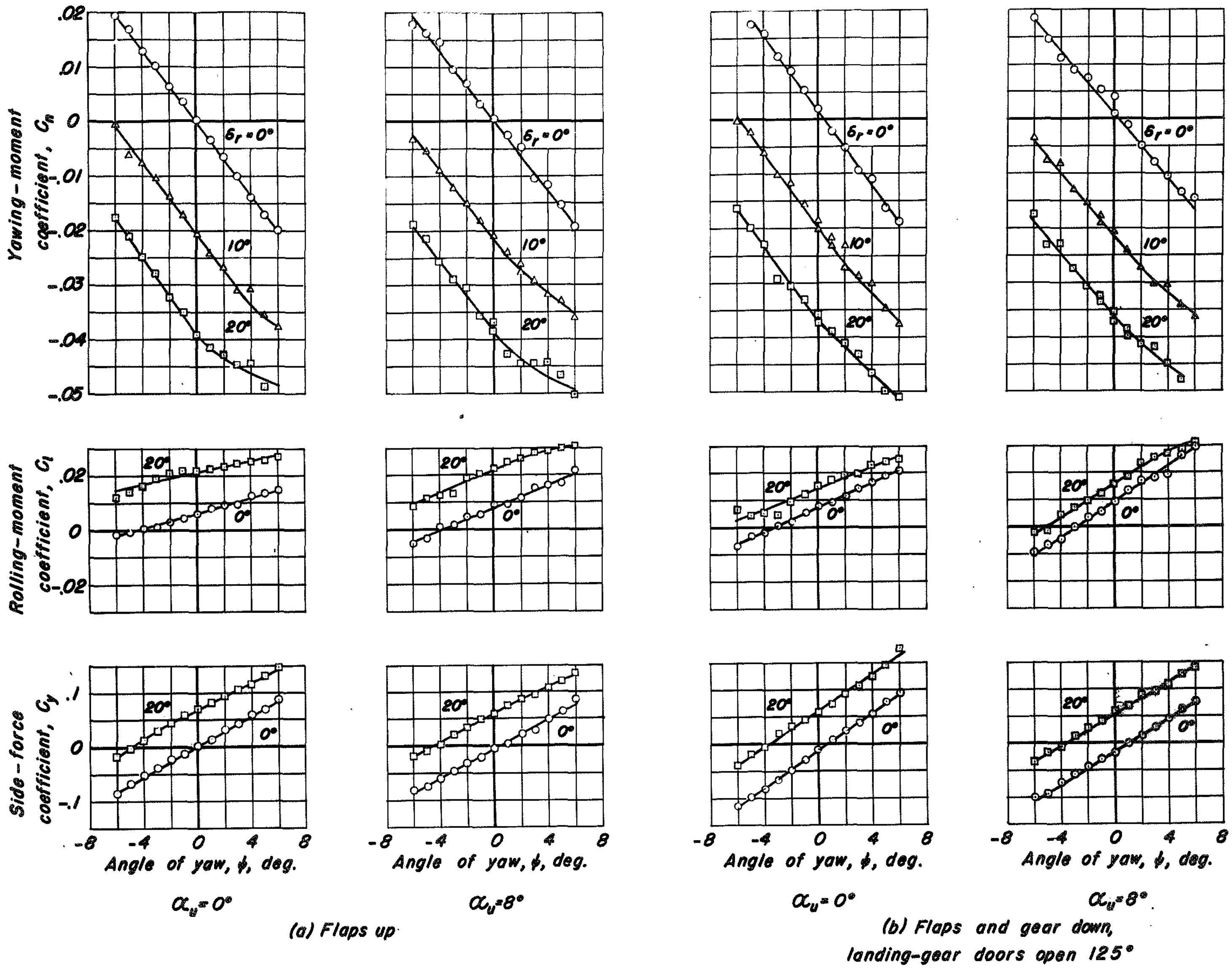

Figure 28.- Effectiveness of the rudder on the conventional tail, drooped wing tips.

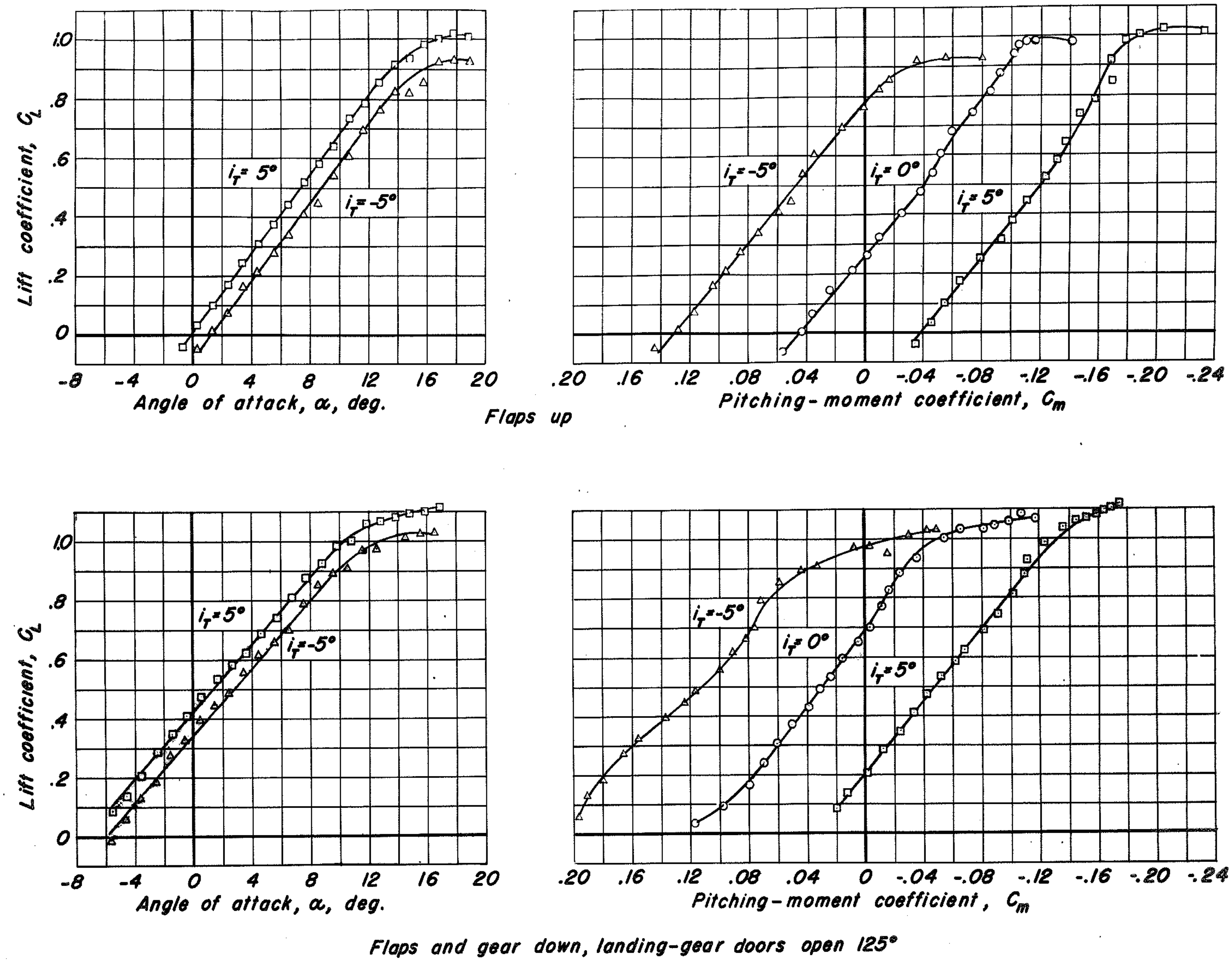

(a) Variation of α and C_m with C_L

Figure 29.- Effect of stabilizer incidence on longitudinal characteristics, drooped wing tips, conventional tail.

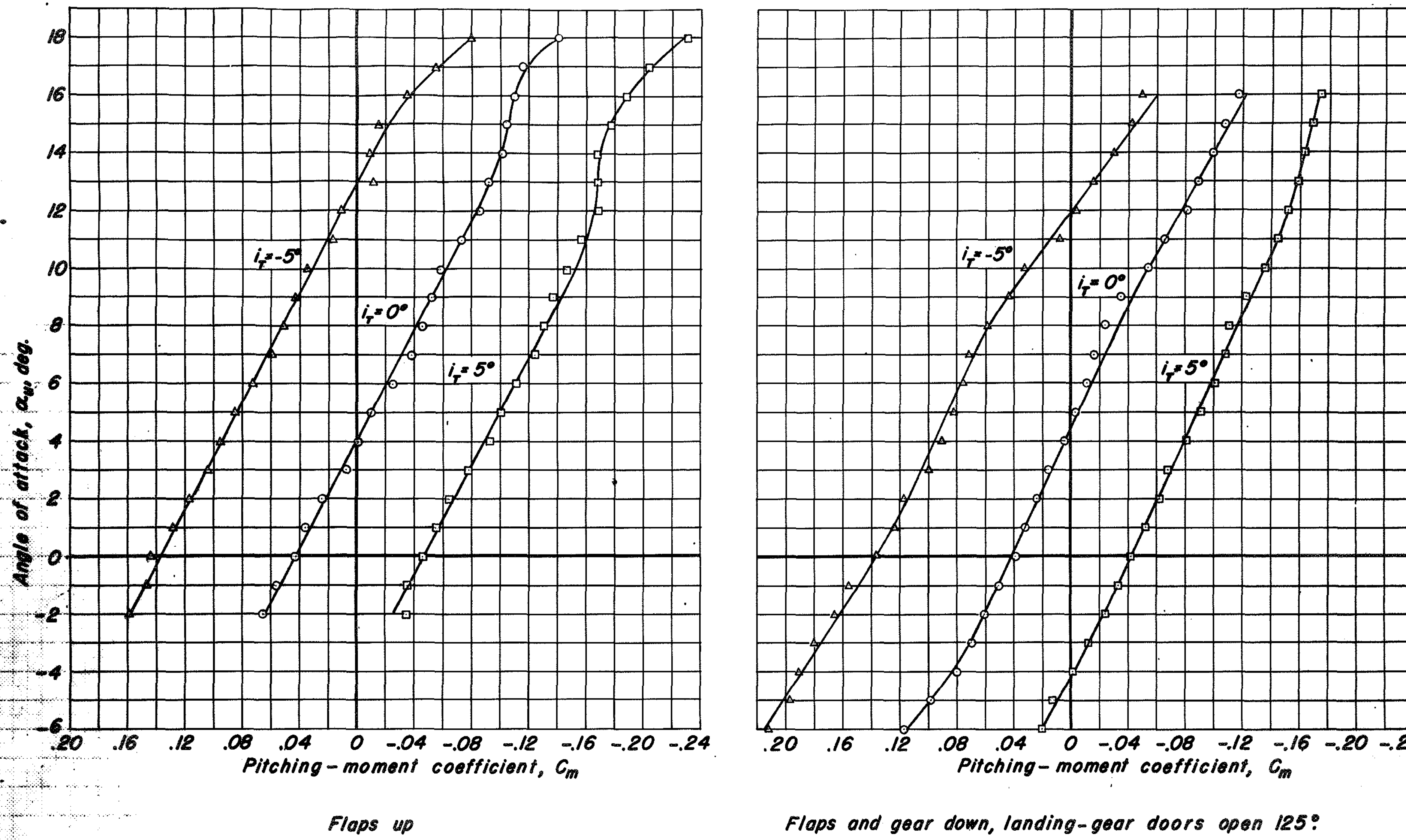

(b) Variation of C_m with α_u

Figure 29.- Concluded.